Chem Soc Rev

# Terpyridine-based Metallosupramolecular Constructs: Tailored Monomers to Precise 2D-Motifs and 3D-metallocages



| | |
|---|---|
| Journal: | *Chemical Society Reviews* |
| Manuscript ID | CS-SYN-01-2018-000030.R2 |
| Article Type: | Review Article |
| Date Submitted by the Author: | 15-Mar-2018 |
| Complete List of Authors: | chakraborty, sourav; University of Akron, Polymer Science<br>Newkome, George; University of Akron, Polymer Science; Florida Atlantic University - John D MacArthur Campus, Center for Molecular Biology and Biotechnology |
| | |

# Terpyridine-Based Metallosupramolecular Constructs: Tailored Monomers to Precise 2D-Motifs and 3D-Metallocages

Sourav Chakraborty*[a] and George R. Newkome*[a,b,c]

[a]*Departments of Polymer Science and* [b]*Chemistry, University of Akron, Akron, Ohio 44325 USA.*
[c]*Center for Molecular Biology and Biotechnology, Florida Atlantic University, Jupiter, Florida 33458, USA.*
E-mail: schakraborty@uakron.edu, newkome@uakron.edu

**Abstract:** This overview represents a comprehensive summary of the recent developments in the growing field of terpyridine-based, discrete metallosupramolecular architectures. The *N*-heteroaromatic ligand [2,2′:6′,2″]terpyridine (tpy) presents a convergent *N,N′,N″*-chelating donor set and has the ability to bind diverse metal ions to form stable pseudo-octahedral <tpy-$M^{2+}$-tpy> bonds. Use of <tpy-$M^{2+}$-tpy> connectivity for the edges and directed organic vertices has opened the door to diverse, dynamic, utilitarian macromolecular materials. New strategies have been employed to synthesize a range of 2D- and 3D-fractals as well as novel macrocyclic constructs by employing new designer strategies, such as: triangle-based frameworks, hexagonal fractal designs, flexible polyterpyridine linkers, and noncovalent interactions for spontaneous quantitative self-assembly. Numerous examples of heteroleptic self-assembly have been described along with the synthesis of heterometallic conjugates using step-wise protocols. Utilizing multiplanar, directed spacer units in the polyterpyridine vertices, new 3D-polyhedra were obtained facilitating the assembly of hybrid fractal-dendritic materials. These constructs are shown to undergo tunable conformational transformations by responding to specific stimuli such as concentration, temperature, and counter ions. The increasing ability to exploit hierarchical self-assembly of complex, higher order supramolecular nanomaterials is discussed.

## 1. Introduction

Nature has always inspired scientists to mimic naturally occurring phenomena to understand basic logical concepts of its functioning and to build extremely complex biosystems from simple precursors. The understanding of Nature's way to organize its building blocks using diverse weak, noncovalent interactions such as hydrogen bonding, ion-dipole, donor-acceptor, π-π, van der Waals, as well as hydrophilic and hydrophobic interactions to achieve very complex architectures paved the way to modern precise supramacromolecular chemistry. Structures with unprecedented complexity and diversity, such as: DNA double helix, secondary and tertiary protein folding, 2D surfaces of lipid bilayer, viral capsids, and micelles have established that very simple monomers can generate exceedingly complicated materials. Early examples of synthetic supramolecular recognition systems were demonstrated by Pederson[1] with the synthesis of crown ethers and encapsulation of selective guest ions, followed by the development of more complex ensembles, such as "cryptands," and "spherands" pioneered by Lehn,[2] and Cram,[3, 4]

respectively, in the area of host-guest assemblies. These discoveries opened to the door to the realization that small complementary molecules can recognize each other using non-covalent interactions to self-assemble into complex supramolecules according to the intrinsic information contained in the monomers. Over the past half century, supramolecular chemistry has grown into an important field of modern science with scientists synthesizing escalating numbers of intricate functional nano-constructs with fascinating chemical and physical properties.[5, 6]

However, with increasing size and degrees-of-complexity, the synthesis of desired large discrete supramolecules becomes very challenging owing to the lack of control over the directionality of most of these noncovalent interactions. The highly directional nature of metal-ligand bonding circumvents difficulties associated with controlling the shape of the desired molecules, afforded by the predictable coordination geometry of transition metal centers. The design and construction of a wide variety of 2D and 3D metallosupramolecular architectures have been achieved *via* coordination driven self-assembly not only because of their artistically pleasing structures but also due to their potential applications in host–guest chemistry, catalysis, sensing, drug delivery, etc.[7-17] Numerous research groups such as: Lehn,[18, 19] Sauvage,[20-22] Stoddart,[12, 23, 24] Stang,[25, 26] Fujita,[27, 28] Newkome,[29, 30] Schmittel,[31, 32] Raymond[9] and others[33-39] individually developed novel coordination paradigms to synthesize many delicate representative molecular constructs such as: helices, grids, knots, polygons, polyhedra, nanospheres etc. of definitive size and shape.[40-49]

Among a wide variety of organic donor ligands, [2,2′:6′,2″]terpyridine (tpy) is ubiquitous as a tridentate, chelating ligand. The use of <tpy-metal-tpy> connectivity of multiterpyridinyl monomers provides the desired synthetic characteristics to facilitate using the metal coordination site to act as edges in designing shapes possessing rigid organic vertices. Terpyridine-based multitopic tectons have gained extensive attention due to their ability to coordinate diverse metals facilitating both labile ($Zn^{2+}$, $Cd^{2+}$) and nonlabile ($Ru^{2+}$, $Os^{2+}$) <tpy-$M^{2+}$-tpy> connectivity, thus permitting control over bond strength and ultimately the desired molecular architecture(s). The criterion of tpy-based assembly is a consequence of both kinetic and thermodynamic control; as for example, kinetically dominated complexation increase in the order $Cd^{2+} < Zn^{2+} < Fe^{2+} < Os^{2+} < Ru^{2+}$.[50] Control over the assembly process is essentially lost when $Os^{2+}$ and $Ru^{2+}$ are employed, due to the kinetic formation of irreversible metal complexes; whereas, $Cd^{2+}$ and $Zn^{2+}$ provide avenues to reversible thermodynamically stable constructs. The interconversion between such thermodynamic and kinetic architectures can only be triggered by appropriate external stimuli, such as: temperature, concentration, and ionic media. The pseudo-octahedral <tpy-$M^{2+}$-tpy> moieties are thus the favorite monomers for diverse metallodendrimers,[51-54] racks,[55, 56] and grids,[57-59] as well as macrocycles, cages and diverse polyhedra.

In this review, the recent progress in the area of terpyridine-based metallosupramolecules is presented with a specific focus on discrete architectures. Although the relevant historical journey of the field is available,[29, 60] an emphasis is placed here on the results achieved over past few years. It is organized to give a brief overview of key structural challenges to design and mimic fractal patterns at the molecular level, as well as highlights its maturation from simple 2D

constructs to higher-dimension complex architectures. The unique concentration-dependent molecular transformations within discrete terpyridine-based supramacromolecules will be emphasized in detail. Moreover, some excellent reviews provide further important insight into specific areas of metallo-terpyridine chemistry, for example Schubert and coworkers extensively reviewed the synthesis, properties and applications of <tpy-$M^{2+}$-tpy>-based metallopolymers and materials.[61, 62] Housecroft and Constable summarized ligand specific perspectives on the coordination behavior of divergent terpyridines for both coordination polymers and discrete systems.[63, 64] A summary of recent developments towards supramolecular polymers, networks, and metallomacrocycles, based on self-assembly of conjugated units using <tpy-$Zn^{2+}$-tpy> connectivity has been presented by Grimsdale *et al*.[65]

Recently, the <tpy-$M^{2+}$-tpy>-based monolayer sheets have gained attention due to their unique properties, derived from two-dimensional polymers. The Schlüter group reported the synthesis of a Zn(II)-based sheet with hexa*kis*terpyridine, followed by site-to-site transmetalation [$Zn^{+2}$ to $Fe^{+2}$, $Co^{+2}$, and $Pb^{+2}$] to form sheets with non-labile metal complexes.[66] Upon complexation with $Mg^{+2}$, a hexathiobenzene functionalized with six peripheral terpyridine results into a 2D-nanosheet with activated phosphorescence in THF. Addition of fluoride ion dissembles the system; thereby switching off the luminescence providing a potential application for fluoride sensing.[67] A series of electrochromic nanosheets comprising of *tris*terpyridine linkers and $Fe^{+2}$ or $Co^{+2}$ was reported by Nishihara *et al*. in which large films of these multilayered 2D coordination nanosheets exhibit rapid and durable electrochromism in an electrolyte solution.[68] We must mentioned here that apart from <tpy-$M^{2+}$-tpy>-based octahedral connectivity, terpyridine-based discrete metallosupramolecular systems of non-octahedral metal centers, such as those of Cu(I),[69, 70] Cu(II),[71-73] Pt(II),[74, 75] Pd(II),[76, 77] and Re(II)[78] have also been reported.

Applications for such tailored-made supramacromolecular compounds[79-81] include host-guest chemistry;[82, 83] light harvesting/emitting;[60, 84, 85], gas storage;[86] sensing[63-65, 87]; waste sequestration;[88] and molecular-scale flasks,[11, 89, 90] electronics,[61,91] molecular antenna[92-94] as well as life science applications, such as DNA binding agent and anticancer therapies.[95-98]

This overview will strictly focus on the design, synthesis, and properties of discrete metallosupramolecules constructed using convergent <tpy-$M^{2+}$-tpy> connectivity. Readers seeking more background knowledge about the origin of terpyridine-based fractal design principles and strategies are directed to our previous reviews.[29, 60]

## 2. Metallomacrocycles and Fractal Architectures

In 1999, the first successful synthesis of a terpyridine-based molecular hexagon by the combination of rigid 120°-bisterpyridine with $RuCl_3$, unveiled the potential of shape-persistent <tpy-$M^{2+}$-tpy> connectivity to ascertain the ease of controlling the shape of the ultimate structures.[99] This observation opened the door to a family of precisely shaped, multi-ionic metallocycles. Expanding on this architectural design principle, the first synthesis of a nondendritic fractal Sierpiński gasket,[100] which incorporates both the "Star of David" as well as a "Kock snowflake" designs, was created via a simple stepwise process (Figure 1). This 2D fractal gasket was assembled in three steps from predesigned terpyridine-based monomers and had a

precise molecular weight of 38,724.38 amu, as pictured in a low temperature STEM. The question is - can such constructs be assembled spontaneously and quantitatively? Thus, can 2D and 3D macromolecular patterns be assembled in one-step from a tailored monomer, as if one would be constructing a building, bridge or work-of-art by combining appropriate substructures but at the nanoscopic level?

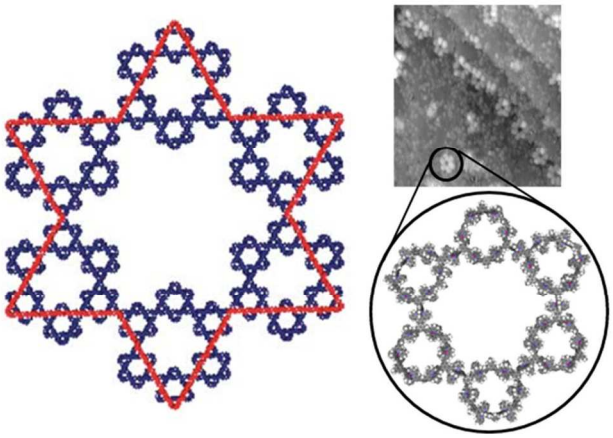

**Figure 1.** Fractal shapes: Sierpiński hexagonal gasket incorporating the "Star of David" and the "Koch snowflake" motifs. Adapted with permission from *Science*, 2006, **312**, 1782-1785 (Copyright 2006 AAAS).

### 2.1. 2D Fractal Architectures

Over the past few years, a synthetic approach using aromatic-based corners with rigid, directed 60° angles to construct new intricate architectures has emerged. A simple chemical palette of related shape-persistent monomers was created, as shown in Figure 2, and used to assemble the organometallic family of simple artistic structures. The monomeric family can be altered by elongation, component substitution, and limited only by one's imagination.

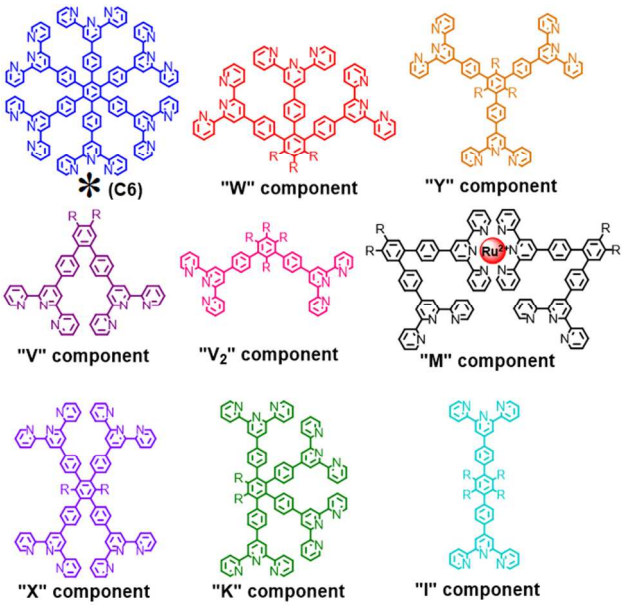

**Figure 2.** A simple artistic palette of possible monomers for assembly.

The triangular shape (as shown in Figure 1) possesses inherent stability, as macroscopically noted in a three-legged stool, and introduces a rigid directed framework upon which large and intricate architectures can be built. This was demonstrated by the self-assembly of the first terpyridine-based, multicomponent, 2D shape-persistent molecular "spoked wheel" (**1**), which can be described as combinations of six equilateral triangles connected facially around a common center (Figure 3).[101] Building on this strategy Lu *et al*. reported the quantitative self-assembly of heteroleptic, centrally fused, rhomboidal structure.[102] Triangular geometry was also employed by Schultz *et al*. in a stepwise assembly of two novel macromolecular constitutional isomers: molecular "bowtie" (**3**) and "butterfly" (**4**) via vertex connectivity;[103] whereas, the rhomboid **2** has interesting structural relationship in that the two triangles are assembled by facial connectivity.

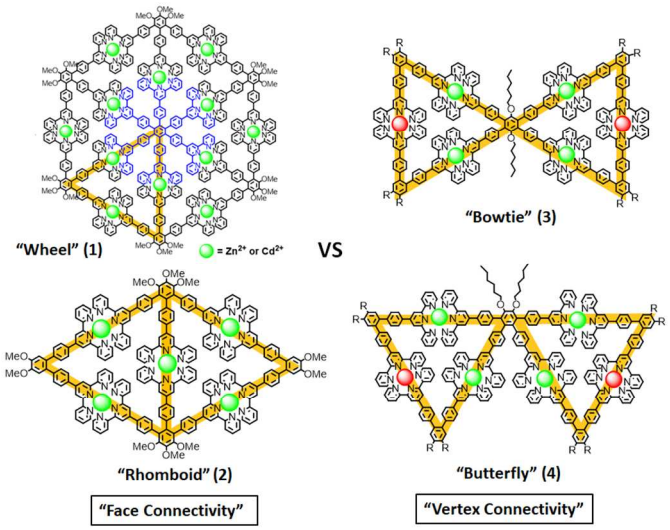


**Figure 3.** Geometric relationships between fractal architectures considering connectivity-directed (vertex vs. face-to-face) assembly of equilateral triangles.

The directed incorporation of triangles has led to the formation of projected structures, opening the door to a more general pathway to high yield syntheses of pure metallofractals, as well as to other interesting architecturally-diverse supramacromolecular constructs. Thus, when a mixture of "V" monomer (**5**) and "K" monomer (**6**) was treated with $Cd^{2+}$ in a precise 1:1:3 stoichiometric ratio, the desired fractal first-generation Sierpiński triangle **7** was created in near quantitative yield.[104] This Sierpiński triangle possessed four triangles with three facial modes of connectivity; whereas, the vertex connectivity is demonstrated by the construction of simple [4]-triangulane (Figure 4).[105] This was accomplished by replacing "K" ligands with three tetratopic "X" units (**8**) for the vertex junctions. The "V" monomer was treated with $Ru(DMSO)_4Cl_2$ to generate the mono$Ru^{2+}$ dimer ("M"), whose conversion to its *bis*-$Ru^{3+}$ adduct followed a known procedure.[100] Treatment of three equiv. of this dimer "M" with the "X" monomer generated **9**, which was followed by self-assembly with three equiv. of $Zn^{2+}$ gave [4]-triangulane (**10**) in quantitative yield. As the size and number of metal ions increased, hydrophobic appendages

were incorporated to increase the overall solubility of the increasingly complex monomers and intermediates.

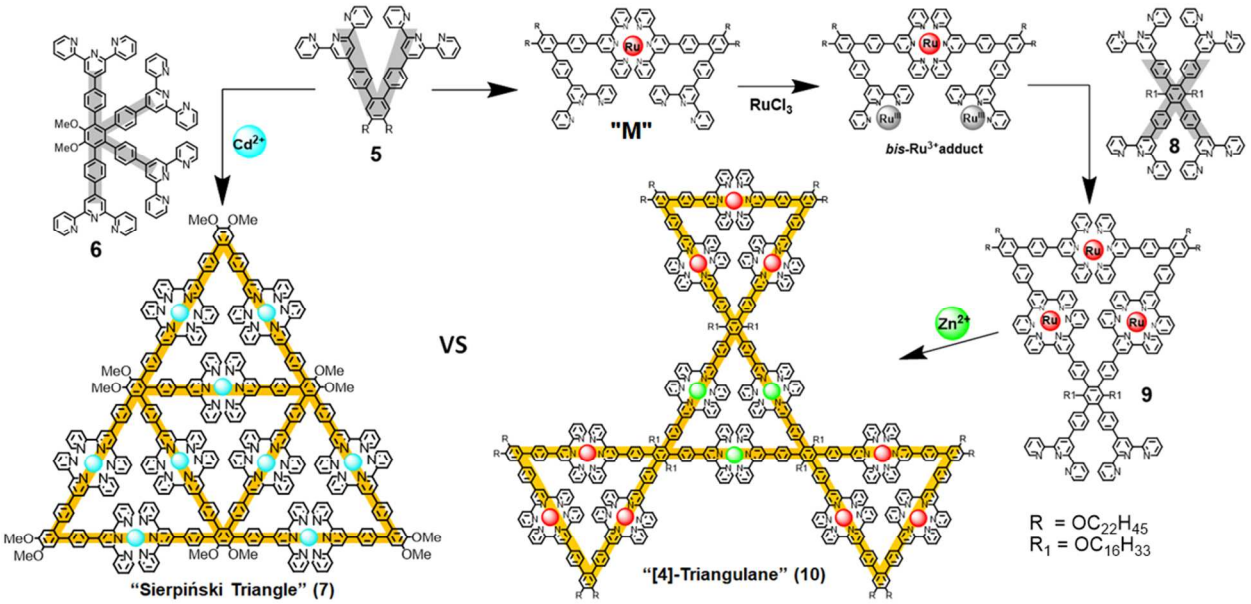


**Figure 4.** Connectivity directed supramolecular isomer Sierpiński triangle and [4]-triangulane. Adapted with permission from *Angew. Chem. Int. Ed.*, 2014, **53**, 12182-12185 and *Eur. J. Org. Chem.* 2016, 5091-5095 (Copyright 2014 and 2016 Wiley-VCH).

A larger saturated Sierpiński triangle was synthesized by combinations of "V" and "K" monomers with a central hexaterpyridine ligand.[106] The corner 60°-*bis*terpyridines ("V"s) were pre-coordinated with two "K" type ligand through stable <tpy-$Ru^{2+}$-tpy> connectivity to generate the metallo-organic monomer **11**. The one-step, self-assembly of three units of **11** with a hexaterpyridine (**C6**) and modes of connectivity lead to **12** (Figure 5) in high overall yield.

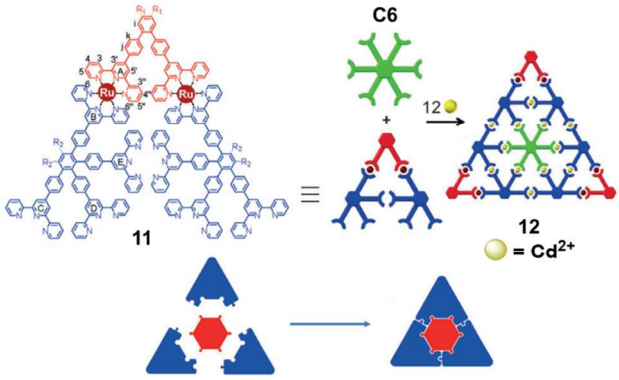


**Figure 5.** Synthetic route towards saturated Sierpiński triangle. Reproduced with permission from *Angew. Chem. Int. Ed.*, 2017, **56**, 11450-11455 (Copyright 2017 Wiley-VCH).

Following this triangle-based fractal architectural design, Wang *et al.* demonstrated the stepwise construction of a supramacromolecular "nut".[107] When the centrally pre-connected monoRu$^{2+}$-dimer (**13**) of 1,2,3-*tris*terpyridine monomer "W", previously shown as the central edge of rhomboid **2**, was treated with the "K" monomer in presence of $Fe^{2+}$, the desired "nut-

like" hexagon **14**, possessing a central hollow Star of David pattern, resulted. This can be viewed as a recursive mathematical form composed of six vertices and six rhomboidal substructures to generate the macrocyclic **14** (Figure 6).

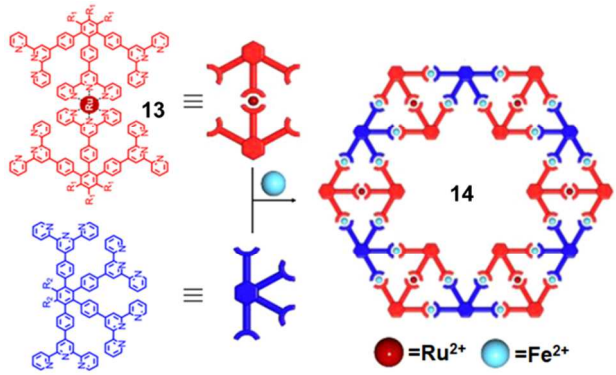


**Figure 6.** Self-assembly of giant hollow hexagonal "nut" **14**. Reproduced with permission from *J. Am. Chem. Soc.*, 2016, **138**, 10041-10046 (Copyright 2016 American Chemical Society).

More recently, the same group reported the stepwise assembly of pentagonal and hexagonal metallosupramolecular architectures with precise star-shaped motifs, using known "V" and "X" monomers.[108] The initial attempt to synthesize the anticipated 6-pointed star **18** using pre-blocked heteroleptic dimer **15** with either $Cd^{2+}$ or $Fe^{2+}$ resulted however, in the generation of an unexpected

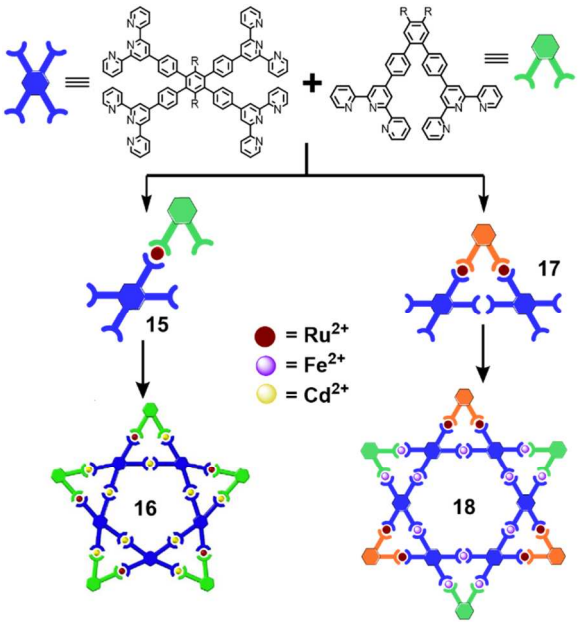


**Figure 7.** Synthetic route towards supramolecular stars **16** and **18**. Adapted from *Nat. Commun.*, 2017, **8**, doi: 10.1038/ncomms15476 (Copyright 2017 Springer Nature).

5-pointed star **16** (Figure 7). The redesigned *bis*$Ru^{2+}$-trimer (**17**) between one "V" and two "X" units, instilled the desired directivity in the monomer; subsequent assembly with three

equivalents of "V" monomer in presence of $Fe^{2+}$ generated the desired Star of David **18,** as shown in AFM and STM.

Utilizing a modular strategy to design and construct tailored metallo-organic monomers, based on stronger <tpy-$Ru^{2+}$-tpy> connectivity, and followed by stepwise synthetic methodology, Zhang *et al*. reported[109] the synthesis of two 2D rhombus star-shaped supramolecules. The ditopic "V" monomer and tritopic "Y" shaped 120°-*tris*terpyridine ligands were bridged through stable <tpy-$Ru^{2+}$-tpy> connectivity as well as directivity into corresponding metal-organic ligands **19** and **20**, respectively; subsequent self-assembly with hexaterpyridine **C6** and $Zn^{2+}$ lead to the formation of the desired "nanosnowflakes" **21** and **22** (Figure 8). The stability of **21** and **22** was further validated by intra- and intermolecular dynamic exchange studies using NMR and mass spectrometry.

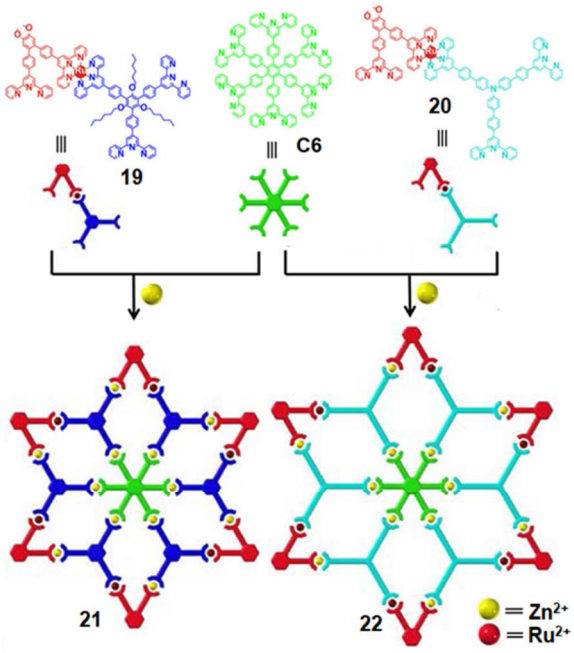


**Figure 8.** Self-assembly of "nanosnowflakes" **21** and **22**. Adapted with permission from *J. Am. Chem. Soc.*, 2017, **139**, 8174–8185 (Copyright 2017 American Chemical Society).

A novel strategy to the one-step self-assembly of fractal architectures without using a 60°-based system was demonstrated by the Li group.[110] To overcome the challenges of conventional self-assembly using the 120°-ditopic *bis*terpyridine, which gives a mixture of metallocycles ($n$ = 5-9) instead of anticipated hexagon,[111-113] they simply increased the density of coordination sites using multitopic ligands. Two supramolecular hexagon "wreaths" (**25** and **26**) were synthesized quantitatively by the self-assembly of the tritopic **23** and tetratopic **24** 120° *bis*terpyridine ligands with $Zn^{2+}$, respectively (Figure 9). The simple image of small hexagons around a central hexagon provided high geometric constraint to exhibit discrete fractal geometry.

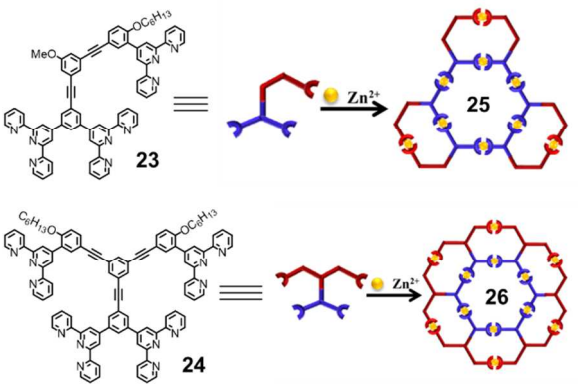


**Figure 9.** Self-assembly of hexagonal wreaths **25** and **26**. Adapted with permission from *J. Am. Chem. Soc.*, 2014, **136**, 6664-6671 (Copyright 2014 American Chemical Society).

Extending this concept of hexagon-based, fractal architectures, the design and construction of a planar supramolecular "honeycomb" fractal were forthcoming.[114] To achieve this goal, the tailored metallo-organic monomer **27**, composed of an inner noncomplexed 120°-*bis*terpyridine and an outer extended free 120°-*bis*terpyridine, linked by three stable <tpy-$Ru^{2+}$-tpy> bonds, was prepared in three steps. The self-assembly of **27** with $Zn^{2+}$ gives the desired **28** (Figure 10) in which the central metallohexagon was surrounded by six identical hexagons that perfectly mimic the simple honeycomb pattern, with an optimized diameter of *ca*. 13.3 nm, which was supported by TEM imaging.

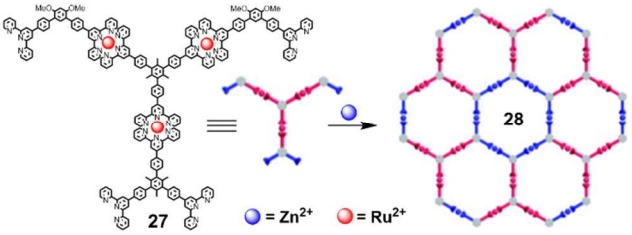


**Figure 10.** Self-assembly of honeycomb pattern **28**. Adapted with permission from *Chem. Commun.*, 2017, **53**, 6732-6735 (Copyright 2014 The Royal Society of Chemistry).

### 2.2. 2D Metallomacrocycles

A report of a series of asymmetric 60°-directed *bis*terpyridine ligands with varying phenyl spacers in both arms has recently appeared.[115] The facile self-assembly of these ligands with labile $Zn^{2+}$ was shown to be highly dependent on the ligand's geometry. The authors found that only one ligand, which has the most pronounced difference in arm length, underwent self-sorting to generate a metallo-triangle with perfect heteroleptic connectivity; other ligands afforded a mixture of constitutional isomers.

Chan *et al.* reported a series of ring-in-ring metallosupramolecular architectures (**29-32**) by using $Cd^{2+}$ and the multivalent terpyridine ligands (**L1-3**) composed of one 60°- and two 120°-directed *bis*terpyridines connected through alkyl chains with varying lengths (Figure 11).[116] Interestingly, variation of alkyl chain lengths within the hexa*kis*terpyridine ligand was shown to control the ultimate shape of the nanoconstructs. The ESI-MS and NMR studies suggest that an

intramolecular complex between two ligands is the key intermediate leading to the desired ring-in-ring structure. By extending the number of coordination sites in the multivalent ligand, the next generation tricyclic superstructure or "spiderweb" pattern was quantitatively produced using the elongated deca*kis*terpyridine ligand. In developing the complementary terpyridine ligand pairing strategy, they also reported the quantitative self-assembly of a heteroleptic ditrigon **33**.[117] The high-fidelity, self-recognition between ligand **L2** and complementary 180°-functionalized *bis*terpyridine **34** lead to the generation of **33**; following the expected incorporation of complimentary units (**34**) into the parallel lateral sides of the previously reported ring-in-ring structure **30** (Figure 11).

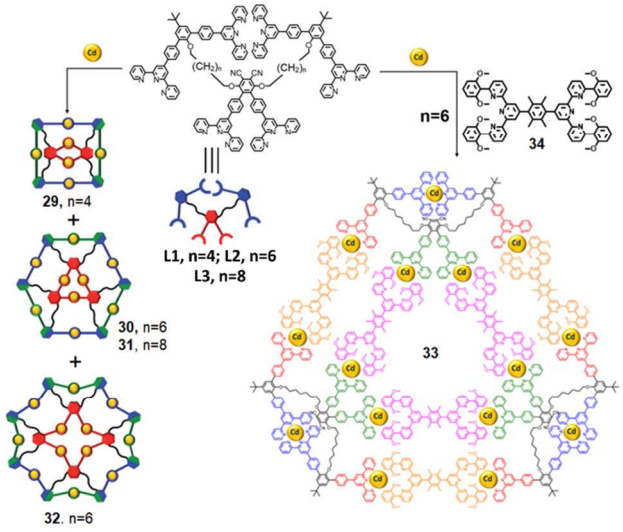


**Figure 11.** Self-assembly of 2D ring-in-ring metallosupramolecular architectures. Adapted with permission from *Angew. Chem. Int. Ed.*, 2015, **54**, 6231-6235 and *J. Am. Chem. Soc.*, 2016, **138**, 3651-3654 (Copyright 2015 Wiley-VCH and 2016 American Chemical Society).

Similarly using a directional bonding strategy, a series of metallosupramolecular hexagonal ring-in-ring structures (**36**) was assembled using tetratopic terpyridine ligands (**35**), which were composed of two extended 120°-*bis*terpyridine units of varying length (Figure 12).[118] The hierarchical self-assembly of these concentric hexagons into ordered "nanoribbons" at a liquid-solid interface was further explored using STM imaging.

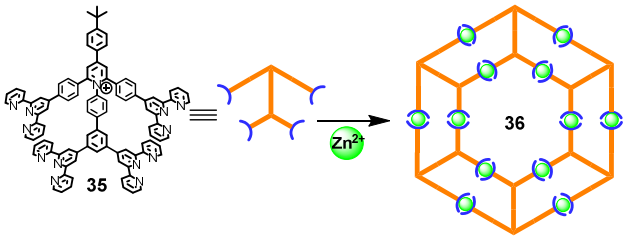


**Figure 12.** Hexagon-in-hexagon structure assembled from tetratopic terpyridine ligands. Adapted with permission from *J. Am. Chem. Soc.*, 2016, **138**, 3651-3654 (2016 American Chemical Society).

Building on 120°-based design strategy the same group recently reported the synthesis of a discrete double-layered hexameric and a triple-layered heptameric rosette type macrocycles

using tetraphenylethylene-based bent tetra*kis*- and hexa*kis*terpyridine linkers, respectively. These rosettes were found to display tunable emissive properties, particularly pure white-light emission for double-layered hexagonal wreath.[119]

Recently, the enhanced formation of selective metallocycles was demonstrated by increasing ligand solubility.[120] The coordination-driven, heteroleptic self-assembly of a tetra*kis*(terpyridinyl)thianthrene with methoxy or benzyloxy functionalized $Ru^{2+}$-dimers of 60°-directed *bis*terpyridine, resulted in a mixture of "bowtie"-shaped macrocycles along with homoleptic tetramers. Increasing the solubility of the Ru-dimer with hexadecyl alkyl chains, the same self-assembly gave exclusively the desired "bowtie"-shaped *bis*-macrocycle. Thus, precise control over the self-assembly processes can be achieved by enhancing the solubility of the intermediates. The effects of increasing the length of alkyl substituents on the topology and metal-ligand connecting nodes in the final assembly of divergent substituted [4,2′:6′,4″]terpyridine ligands have been well-demonstrated by the notable works of Constable and coworkers.[121-123]

Previously, Newkome *et al*. reported the complexation of carbazole-based *bis*terpyridine ligands with a 105° bite angle with nonlabile metal ions to form metallopentacycles.[124] Recently, the self-assembly of two modified carbazole-based ligands, having longer terpyridine arms, was revisited to measure the effects of solubility and *H*-bonding on the assembly process.[125] The self-assembly of non-alkylated parent carbazole ligand (N-H ligand) showed clean formation of the pentameric macrocycle; whereas, analogous attempt with *N*-dodecyl variants resulted in a mixture of macrocycles. Contrary to the previous observations, where increasing solubility facilitated the selective assembly, in this case the lack of *H*-bonding for dodecyl-functionalized species increased the likelihood of an equilibrium mixture.

In an attempt towards creating molecular Borromean links, Siegel *et al.* reported the stepwise synthesis of a new flexible ring-in-ring threading structure **37**, anchored together through <tpy-$Ru^{2+}$-tpy> connectivity (Figure 13).[126] This two-ring structure contained two open terpyridine caps within the inner ring, providing sites to incorporate the third missing ring to complete the Borromean links. Extending this synthetic methodology and using specially designed directional building blocks, based on modified [2,2′:6′,2″]terpyridine connectivity, they have reported the mass spectrometric evidence for the formation of ruthenium(II) complex, molecular Borromean links **38**, consisting of three unequal rings (Figure 13).[127]

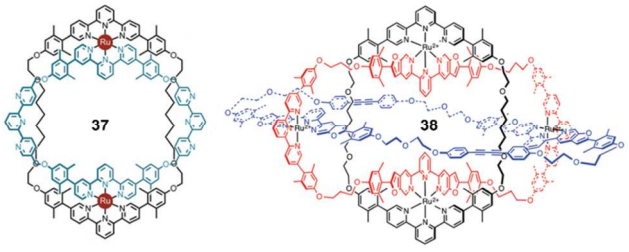


**Figure13.** Ring-in-ring structure **37** and Borromean links **38**. Reproduced from *Org. Chem. Front.*, 2016, **3**, 661-666 and *Org. Chem. Front.*, 2016, **3**, 667-672 (Copyright 2016 The Royal Society of Chemistry).

Both *cis*- and *trans*-isomers of an azobenzene-linked *bis*-terpyridine were incorporated into a discrete macrocycle through <tpy-$Fe^{2+}$-tpy> connectivity.[128] While the extended *trans*-isomer forms a dinuclear macrocycle, the shorter *cis*-isomer forms a mononuclear $Fe^{II}$-complex, which was not only thermally stable but also photochemically inactive. This result indicated a perfect dual locking of photo- and thermal isomerization of *cis*-azobenzene.

The facile heteroleptic assembly of a trapezoid-shaped macrocycle **41** was achieved from designer polyterpyridine metallo-organic monomers (**39** and **40**) using three different <tpy-$M^{2+}$-tpy> bonds ($M^{2+}$ = $Ru^{2+}$, $Fe^{2+}$, $Zn^{2+}$) within a single macrocyclic ring (Figure 14).[129] This trimetallic macrocycle introduced the construction of polymetallosupramolecular assemblies possessing multiple, differing metal centers in predetermined patterns. The successful preparation of this multi-metallic, discrete architecture demonstrated the ease of access to synthesize new interesting structural and chemical possibilities by logically positioning, different <tpy-$M^{2+}$-tpy> linkages within a custom-designed framework. This also opens the door for instilling site-specific metal centers within an electronically interconnected framework.

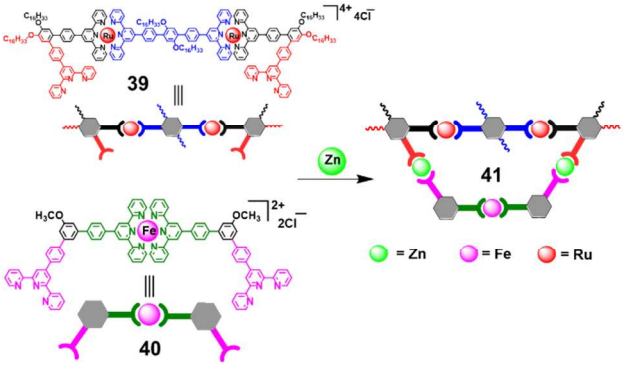


**Figure 14.** Synthesis of molecular trapezoid **41** possessing three different metals. Reproduced with permission from *Chem. Commun.*, 2017, **53**, 8038-8041 (Copyright 2017 The Royal Society of Chemistry).

Combining edge- and vertex-directed coordination bonding approaches, heteroleptic assemblies can also be achieved by using heterotopic ligands in which two different binding sites prefer entirely different metal ions. Thus, 4'-(3-pyridyl)[2,2':6',2"]terpyridine was used to form metalloligand **42** by complexation with $Fe^{2+}$ or $Ru^{2+}$; self-assembly of **42** with a *trans*-Pd(II) acceptor linker using the free pyridine forms hexanuclear triangular metallocycle **43** (Figure 15). The photophysical and electrochemical properties of the resulting multicomponent metallocycle was explored and it exhibited a multi-electronic redox process with negligible communication among metal centers.[130]

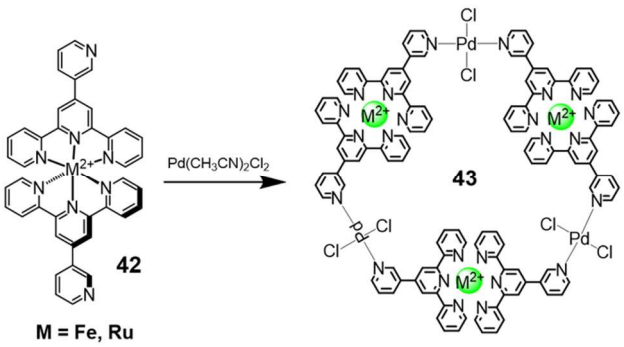


**Figure 15.** Self-assembly of heterometallic Pd(II)/Fe(II) and Pd(II)/Ru(II) macrocycles *via* precoordinated terpyridine metalloligand. Adapted with permission from *RSC Advances*, 2014, **4**, 21262-21266 (Copyright 2014 The Royal Society of Chemistry).

Self-assembly between similar terpyridine-based metalloligands (M = $Zn^{+2}$, $Ni^{+2}$, $Cu^{+2}$) with 4-pyridyl terminal moieties and half-sandwich organometallic acceptor clips [($Cp^*_2M_2$(μ-DHNA)$Cl_2$] (M = $Ir^+$ and $Rh^+$; Cp* = $\eta^5$-pentamethylcyclopentadienyl; DHNA = 6,11-dihydroxy-5,12-naphthacenedione) led to the formation of a series of hexanuclear heterometallic box-type macrocycles. Interestingly, the iridium metallocycles selectively encapsulate two triflate guests within their molecular cavities; whereas in all other cases, the counterions exist outside the molecular backbones.[131]

Further extending this novel heteroleptic multicomponent self-assembly approach, Stang *et al.* reported[132] the synthesis of two unprecedented heterometallic bicyclic architectures by using a mono-terpyridine ligand with two 3-pyridinyl termini. The self-assembly of the $Fe^{2+}$-dimer **44** with linear ditopic $Pt^{+2}$-acceptor and a *bis*-pyridine donor facilitated the construction of heteroleptic bicyclic architectures **45** and **46** (Figure 16), comprised of two twisted irregular hexagons joined *via* stable <tpy-$Fe^{2+}$-tpy> hinges.

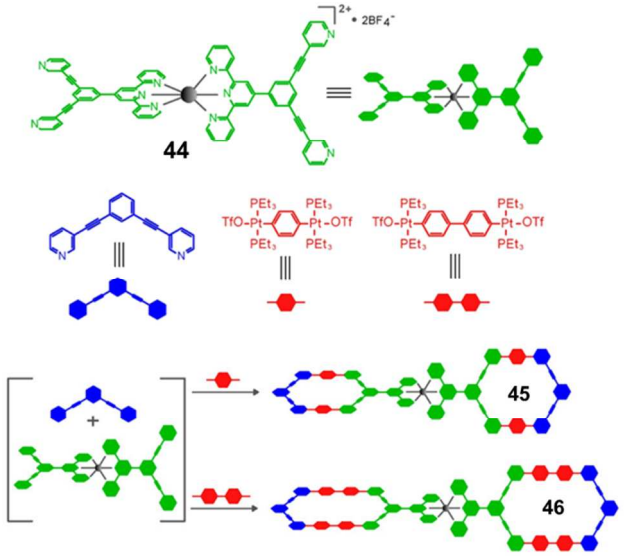


**Figure 16.** Synthesis of terpyridine-based metalloligand **44** and the self-assembly of Fe-Pt twisted heterometallic bicyclic supramolecules. Adapted with permission from *J. Am. Chem. Soc.*, 2017, **139**, 2553-2556 (Copyright 2017 American Chemical Society).

### 3. 3D Fractals and Cages

Self-assemblies of highly symmetric polyhedral cage-like structures, such as viral capsids[133] and protein transport complexes COP I and COP II[134], are abundant in Nature. Replicating such complex architectures is synthetically challenging owing to, in part, the need for precise control over geometry of the building blocks. Highly directional metal-ligand coordination bonds provide some structural control in order to carefully design the ligand's geometric requirements. This paved the way to various 3D metallosupramolecular structures, ranging from simple Platonic solids to complex Archimedean geometries. Different approaches have been employed for the construction of 3D architectures using <tpy-$M^{2+}$-tpy> connectivity. They include angular diversion by *meta*-substituted phenyl spacers, multiple plane-of-directionality using rigid three-dimensional vertices (*e.g.*: adamantane, triptycene, 9,10-ethanoanthracene, *etc*.), and combining directionality with flexible vertices and steric overlap.

The earliest example of a self-assembled terpyridine-based hexameric 3D cage was realized by combining a tetratopic terpyridine functionalized cavitands with $Zn^{2+}$.[135] Early examples of terpyridine-based 3D constructs were derived from molecularly distorted monomers; thus, when the hexameric core of the original molecular "spoked wheel" **1** (Figure 2 above) was replaced with two equivalents of 1,3,5-*tris*terpyridine ligand **S3** ("Y" monomer), a three-dimensional spoked "bicyclic wheel" **47** was devised (Figure 17).[136] A stacked pair of opposite directed *tris*linkers provide the six "spokes" and six 1,2,3-*tris*linker **R3** ("W" monomer) generate the hexagonal rim. The central two 120° *tris*-ligands are stacked with a common perpendicular axis to form a quasi-hexa*kis*-ligand, which imparts the 3D "bicycle-wheel" framework. Similarly, two equivalents of the rim's "W" component can also be used to generate the *bis*-rhomboidal shaped core, which can align with the other rim components; thus, it can play dual roles as both the rim and core. Thus, the homoleptic assembly of eight "W" monomers (**R3**) with 12 $Zn^{2+}$ generate a *bis*-rhomboidal-shaped, three-dimensional molecular "wheel" **48** (Figure 17).[137]

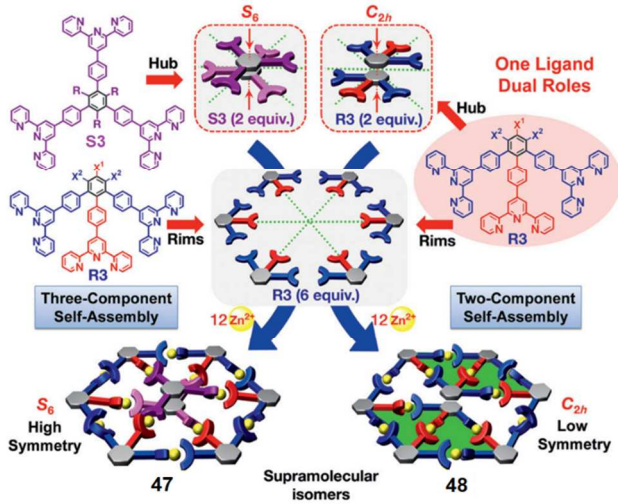


**Figure 17.** Pictorial assembly of the supramolecular 3D wheels **47** and **48**. Reproduced with permission from *Chem. Eur. J.*, 2014, **20**, 13094-13098 (Copyright 2014 Wiley-VCH).

Introducing a new twist using *meta*-substitution along the phenyl spacers of ligands, a three-dimensional, highly symmetric, terpyridine-based nanosphere was created.[138] Thus, when *tris*(4-bromophenyl)benzene was treated with 3′-boronatophenyl[2,2′:6′,2″]terpyridine, the novel *tris*terpyridine monomer **49** was obtained. The coordination of four **49** with six $Ru^{2+}$ gave rise to the nanosphere **50**, as a red solid. The 1,3-disubstituted phenyl spacer instilled the appropriate angle necessary for the monomer to adopt the observed pseudooctahedral geometry (Figure 18). The presence of hexaRu connectivity facilitated the exceptional stability of complex **50** over a wide range of pH values (1-14). Further applying this *meta*-substituted design strategy and utilizing a hexapodal, branched terpyridine ligand instead of the *tris*terpyridine ligand, Wang and coworkers reported the synthesis of a tetrameric metallo-nanosphere and explored their hierarchically self-assembly into berry-type nanostructures.[139]

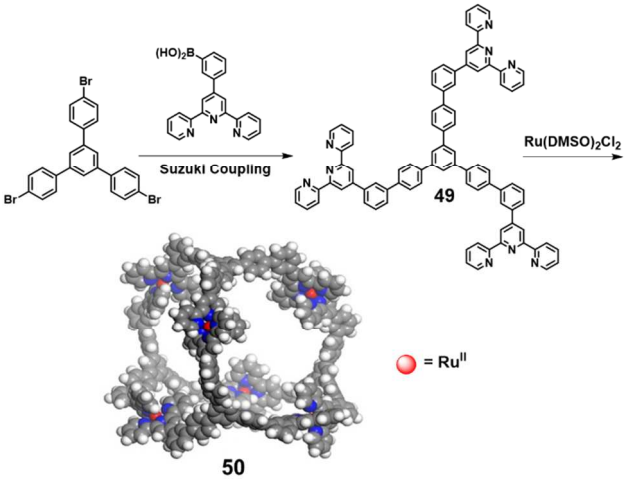


**Figure 18.** Synthesis of the $Ru^{2+}$-Based, metallo-nanosphere **50**. Adapted with permission from *J. Am. Chem. Soc.*, 2014, **136**, 8165-8168 (Copyright 2014 American Chemical Society).

The design and construction of the first multicomponent stepwise assembly of a three-dimensional "propeller"-shaped metallotricyclic spirane were recently reported.[140] The synthetic steps involved the dimerization of a 60°-*bis*terpyridine ligand to give a mono$Ru^{2+}$-dimer, which formed the outer rims of the metallospirane; the synthesis of corresponding $RuCl_3$ adduct **51** followed a known procedure.[100] Treatment of **51** with the 3D hexa*kis*terpyridinyl triptycene core **52** [derived by a six-fold Suzuki-coupling reaction between the hexabromotriptycene and (4'-terpyridinyl)-4-phenylboronic acid, under reducing conditions] gave the desired *tris*macrocycle **53** (Figure 19). The 3D triptycene core enforces three different planes-of-directionality from which the "propeller" shape arises.

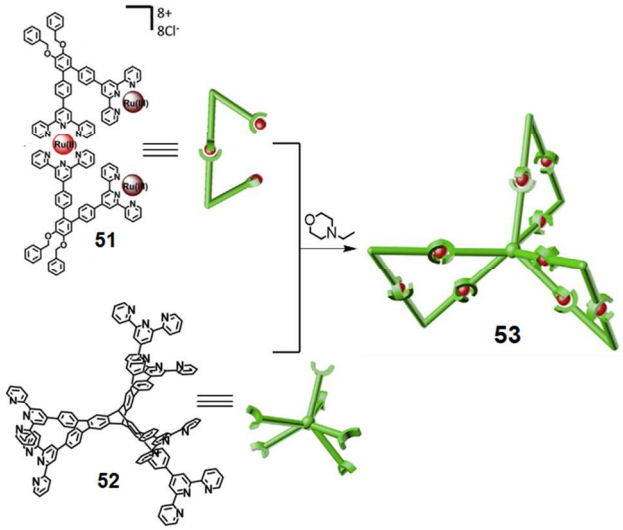


**Figure 19.** Stepwise multicomponent assembly of the propeller shaped metallotricyclic spirane. Adapted with permission from *Chem. Eur. J.*, 2014, **20**, 11291-11294 (Copyright 2014 Wiley-VCH).

The synthesis of a metallosupramolecular cube has been demonstrated using adamantoid-based *tris*terpyridine ligands.[141] The tritopic ligands were constructed on an adamantane vertex to provide three planes possessing 109° directionality; however during self-assembly, these terpyridine arms adopt the critical 90° directionality to generate the desired cubic structure in quantitative yield. Varying the arm length and directionality via either a thiophene spacer or *meta*-phenyl spacer, two other adamantoid-based *tris*terpyridine ligands were synthesized; their self-assembly with $Zn^{2+}$ gave rise to tetrameric and dimeric cages, respectively.[142] From these observations, it has been concluded that the angle between the adamantane core and the terpyridine coordination site plays a critical role in guiding the formation of such assembled structures.

Following the directional-bonding approach, the relative bite angles between terpyridine terminals and the use of equilibrating metals ions are key factors for the design of novel three-dimensional architectures. This has been demonstrated by the synthesis of an Archimedean polyhedron using tetra*kis*terpyridine **54**, which contains both the 60° and 90° directionality so critical for the generation of metallocuboctahedron **55** upon self-assembly with $Zn^{2+}$ (Figure 20).[143] The shape of this giant molecular sphere was unequivocally characterized by synchrotron X-ray analysis. When $Cd^{+2}$ was used in the assembly process, the related cuboctahedron (**56**) was generated and shown to undergo an interesting and previously unobserved concentration-dependent structural interconversion, which will be discussed in the following section.

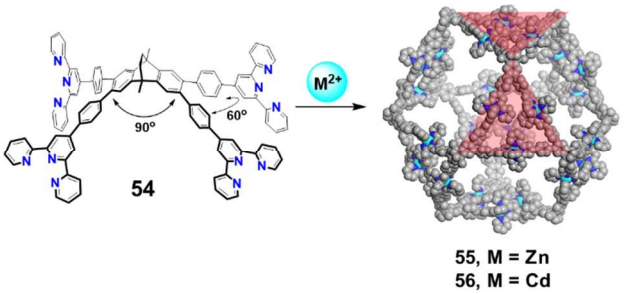


**Figure 20.** Self-assembly of $Zn^{2+}$- and $Cd^{2+}$-based metallocuboctahedron. Adapted with permission from *Angew. Chem. Int. Ed.*, 2015, **54**, 9224-9229 (Copyright 2015 Wiley-VCH).

Most of the terpyridine-based monomers used to design discrete structures have possessed a rigid geometry, because the instilled directionality of terpyridine terminals is critical to attain the desired predictable geometry. Only a handful of flexible terpyridine ligands[144-147] has been used so-far for this purpose and generally under high dilution conditions.[148] Macrocyclization using such flexible linkers generally resulted in forming metallosupramolecular polymers. The same methodology has also been used for intramolecular macrocyclization generating spirometallo-dendrimers.[149]

Using the strategy of "directed flexibility," a 3D polygon was achieved by connecting a trio of 60° *bis*-ligands with flexible crown ether vertices.[150] The tribenzo-27-crown-9 ether, functionalized with six phenylterpyridines (**57)**, was synthesized in six steps and subsequent self-assembly with $Zn^{2+}$ to generate an extended tetrahedron **58**, which is comprised of four independent triangular surfaces interlinked by crown ether vertices (Figure 21). The flexible crown ether vertices allow the extension of highly directed *bis*-ligands to form the triangular planes of directionality facilitated by intramolecular π–π interactions, which ultimately gave the 3D architecture. The host-guest interaction of tetrahedron **58** with tetra*kis*[3,5-*bis*(trifluoromethyl)phenyl]borate (BARF) counterion was probed using $^{19}F$ NMR spectroscopy.

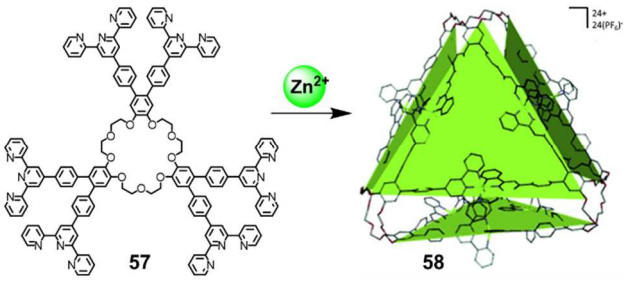


**Figure 21.** Self-assembly of extended tetrahedron structure **58**. The structure's four independent triangles are highlighted in green to aid in visualization of the structure. Reproduced with permission from *Chem. Commun.*, 2015, **51**, 3820-3823 (Copyright 2015 The Royal Society of Chemistry).

Following this strategy of balancing directionality and flexibility, two hexanuclear superposed *bis*-triangle/metalloprisms possessing three dibenzo[24]crown-8 vertices were synthesized using tetratopic terpyridine ligand **59**.[151] The presence of a more flexible larger crown-8 component allowed the linker to adopt a 0° dihedral angle between both the 60° *bis*-terpyridine units, thus facilitating the formation of metalloprisms **60** and **61** in quantitative yield.

These prismatic cages act as a host to encapsulate a predesigned guest molecule **TriG**, possessing dibenzylammonium ions, to afford the corresponding metallosupramolecular host-guest complex pseudosuit[3]anes (Figure 22). The guest inclusion rate was found to be depend on the extent of dynamic nature of metal-ligand coordination bond, leading to a selective guest encapsulation with $Cd^{2+}$-cage **61** in presence of $Zn^{2+}$-metalloprism **60**.

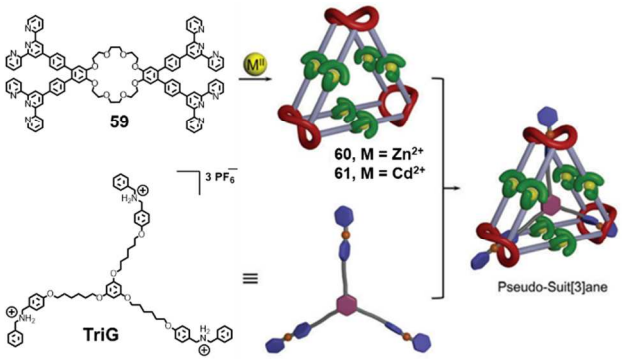


**Figure 22.** Self-assembly of metalloprism and guest (TriG) induce assembly of a metallo-supramolecular pseudosuit[3]ane. Reproduced with permission from *Chem. Commun.*, 2016, **52**, 12622-12625 (Copyright 2016 The Royal Society of Chemistry).

In an aim to incorporate diverse functional scaffolds into shape-persistent, terpyridine-based architectures, the synthesis of a polycyclic, porphyrin-based nanobelt[152] was recently reported. The novel tetra*kis*terpyridinyl-substituted porphyrin (**62**), possessing *meta*-substituted phenyl spacer groups, underwent self-assembly to generate a 3D, belt-shaped metallomacrocycle **63**, which was characterized by multinuclear NMR spectroscopy and ion mobility mass spectrometry (Figure 23).

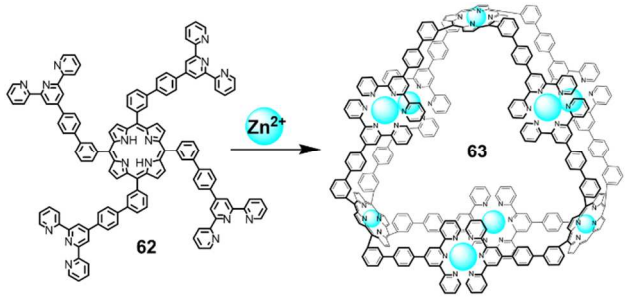


**Figure 23.** Self-assembly of porphyrin-based metallomacrocyclic nanobelt. Adapted with permission from *J. Inorg. Organomet. Polym. Mater.*, 2016, **26**, 907-913 (Copyright 2016 Springer Nature).

A series of metallomacrocyclic tetramers has been synthesized by employing a 60° *bis*terpyridine ligand. Owing to its unique folded 3D architecture, the descriptive term "Dondorff Rings" was coined.[153] This approach to 3D macrocycles was accomplished by the synthesis of a 60°-oriented hexamer using a designer *bis*-ligand.[154] By applying the multicomponent self-assembly strategy using the vertex- and edge-directed bonding approaches, the construction of heteroleptic 3D assemblies was accomplished.[155] The planar <tpy-$Ru^{2+}$-tpy> metalloligand, decorated with four pendent 4-pyridyl terminal donor moieties, self-assembled using the *cis*-protected square-planer $Pd^{+2}$-acceptor linker to form bimetallic tetrameric cage **64** (Figure 24).

The introduction of an ethynyl spacer between pyridine donor and metalloligand backbone resulted in the formation of a smaller trimeric trigonal prism-shaped cage **65**, highlighting the effect of size and flexibility of the linker on the self-assembly process.

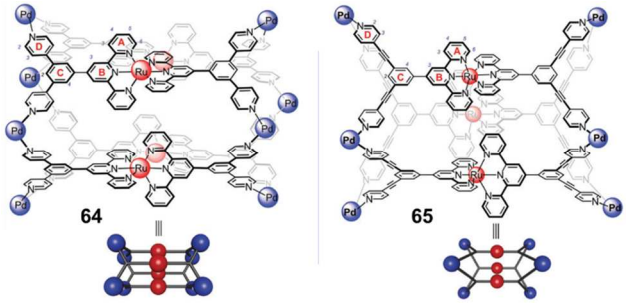


**Figure 24.** Synthesis of heterometallic Pd/Ru molecular cages *via* precoordinated terpyridine metalloligand. Reproduced with permission from *Chem. Commun.*, 2015, **51**, 4465-4468 (Copyright 2015 The Royal Society of Chemistry).

More recently, the synthesis of a series of dinuclear <tpy-$Ru^{+2}$-tpy> complexes possessing two pyridine donor terminals was reported.[156] The combination of one of the dinuclear <tpy-$Ru^{2+}$-tpy> metal complexes with Pd(II) leads to the formation of a tetrameric heteroleptic molecular cage, which was well characterized by NMR and ESI-MS spectrometry. The visualization of the shape of the construct was achieved by computer generated molecular modelling. Apart from the above examples several planar polyterpyridine ligands have been used in conjugation with other ligands to build trigonal prisms in a heteroleptic system.[157]

## 4. Metallosupramolecular Interconversions

Within biological systems, cell growth and cell division are complex endeavors that occur in a very routine, precise manner within each living organism. Fundamental biomolecules undergo molecular folding, structural rearrangement, and subcomponent association to play an important role in molecular recognition, catalysis, and biological processes.[158-160] Probing the precise control over the interconversion between different supramolecular assemblies is challenging since generally mixtures or polymeric materials are the result. The dynamic nature of the non-covalent supramolecular interactions can facilitate disassembly-reassembly of the molecular components. Relatively rigid, yet dynamic coordination bonding, provides a unique blend for metallosupra-molecular interconversions. Diverse factors, such as solvents, concentration, anions, guests, addition of new components, light, temperature, and postsynthetic modifications have been successfully employed to activate molecular transformations, resulting in new species with different functions and properties.[161]

### 4.1 Concentration (or counterion) induced supramolecular transformations

In 1996, Fujita *et al.* first reported the triangle–square equilibrium of metallacycles,[162] in which a dynamic equilibrium between multiple discrete metallosupramolecules in solution was observed. More recently, the self-assembly of an *o*-carborane-based, *bis*terpyridinyl ligand **66** with $Zn^{2+}$ revealed a concentration-dependent dynamic equilibrium between dimer **67** and trimer **68** along with minor tetramer species **69** (detected by ESI-MS only).[163] This concentration-dependent interconversion between dimer and trimer was probed by ESI-MS and NMR studies. Upon dilution, the equilibrium shifts toward the entropically favored dimer **67** (Figure 25), which was obtained exclusively at concentration 20 μg $mL^{-1}$.

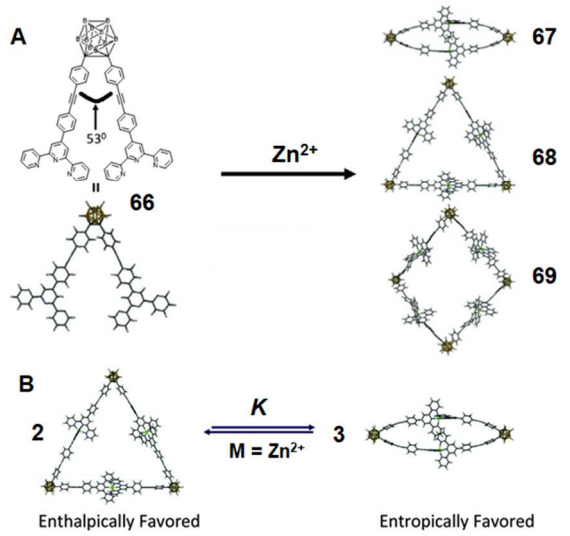


**Figure 25.** (A) Synthesis of carborane functionalized dimeric, trimeric and tetrameric macrocycles. (B) Equilibrium between trimer (**68**) and dimer (**67**). Reproduced with permission from *Dalton Trans.*, 2014, **43**, 9604-9611 (Copyright 2014 The Royal Society of Chemistry).

As introduced above, ring-in-ring *bis*macrocycles were generated by assembling $Cd^{2+}$ ions and multivalent terpyridine linker with varying alkyl linkages.[116] The self-assembly of ligands bearing C4 and C8 alkyl linkers results into the formation of ring-in-ring macrocycles **29** and **31**, as the sole isolated product (Figure 11). Whereas, in case of ligand **L2** with six methylene linkers, the same self-assembly procedure afforded a concentration-dependent dynamic equilibrium between trimer□hexamer **30** and tetramer□octamer **32** (Figure 26). While at low concentration **30** was observed as the sole product; the proportion of complex **32** was found to be predominant at a higher concentration.

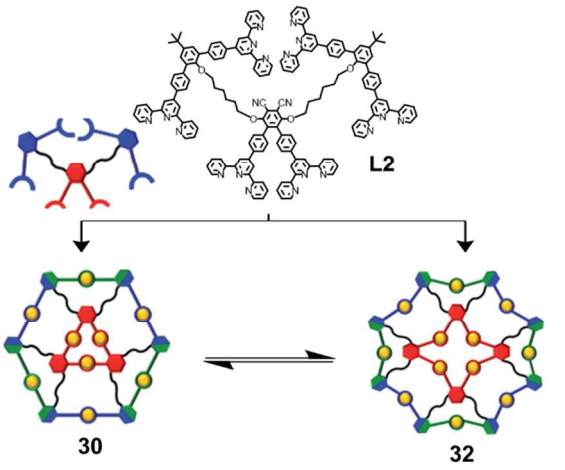


**Figure 26.** Concentration-dependent dynamic equilibrium between trimer□hexamer **30** and tetramer□octamer **32** macrocycles. Adapted with permission from *Angew. Chem. Int. Ed.*, 2015, **54**, 6231-6235 (Copyright 2015 Wiley-VCH).

Following the observation of dynamic equilibrium between terpyridine-based 2D constructs, the first example of a novel concentration-dependent, precise molecular transformation between two three-dimensional metallosupramolecular architectures, a *bis*-rhombus **70** and a tetrahedron **71** was observed (Figure 27).[164] At a concentration higher than 12 mg $mL^{-1}$, the self-assembly of a two-dimensional *tris*terpyridine monomer **R3** with $Cd^{2+}$ in 2:3 ratio resulted in the formation of the *bis*-rhombus **70** in accordance to the previously reported complexation system (**48**) with $Zn^{2+}$.[137] After **70** was fully characterized, the characterization was repeated after dilution. Upon sufficient dilution (0.5 mg $mL^{-1}$), **70** undergoes a spontaneous fission to generate exactly two equivalents of $S_4$ symmetric tetrahedron **71**, which was characterized and shown to be precisely one half of the original molecular weight. Upon attempted isolation, this tetrahedron underwent conversion back to the original *bis*-rhombus. This observation opens a Pandora's box for unusual chemical pathways to unexpected molecular constructs, based on different concentration conditions.

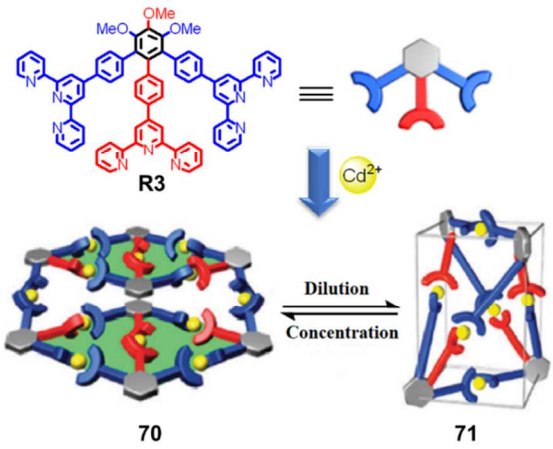

**Figure 27.** Concentration dependent reversible metallosupramolecular transformation between *bis*-rhombus **70** and tetrahedron **71**. Adapted with permission from *J. Am. Chem. Soc.*, 2014, **136**, 18149-18155 (Copyright 2014 American Chemical Society).

In quest of new molecular designs and construction routes to new materials, structural inspiration can often be obtained by looking at new building designs or from the world-of-art, *e.g.*, Cézanne's oil on canvas - the "*Harlequin.*" The intrinsic bite angle and directivity of terpyridine terminals in combination with the appropriate equilibrating metal atoms are critical to obtain a desired molecular architecture. As mentioned above, the single step, quantitative self-assembly of shape-persistent Archimedean-based tetra*kis*terpyridine building block **54** with $Zn^{2+}$ in precise 1:2 ratio, generated the desired metallocuboctahedron **55**.[143] The related $Cd^{2+}$ cuboctahedron **56**, possessing the more labile <tpy-$Cd^{2+}$-tpy> connectivity and $PF_6^-$ counterions, was shown to undergo concentration-dependent dynamic molecular interconversion into exactly two equivalents of octahedron **72** in dilute solution; and increasing the concentration reverses the process regenerating the cuboctahedron (Figure 28). The reversibility of this transformation was probed with NMR and ESI-MS analysis and interestingly; there is no analytical evidence for any other intermediate(s) during this interconversion. Notably, the use of different sized counterions can also play an important role on the overall structural stability. Thus, when the larger counterion $BPh_4^-$ was used instead of $PF_6^-$, the system gave only the octahedral structure.

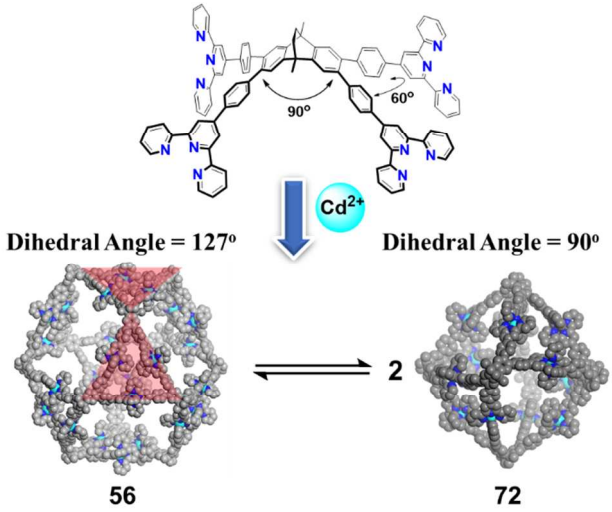


**Figure 28.** Precise Molecular Fission and Fusion between the cuboctahedron and octahedron. Adapted with permission from *Angew. Chem. Int. Ed.*, 2015, **54**, 9224-9229 (Copyright 2015 Wiley-VCH).

The extent of flexibility depends on the degrees-of-freedom associated with the size of crown ethers, which ultimately plays an important role for selective formation of 3D structures. While, the formation of hexanuclear metalloprisms was the logical outcome for self-assembly of a dibenzo[24]crown-8 based tetra*kis*terpyridine ligand,[151] the replacement of the crown part with a smaller dibenzo[18]crown-6 facilitates the formation of a giant metallocuboctahedron that is composed of 12 ligands and 24 metal ions.[165] The quantitative self-assembly of a shape-persistent tetra*kis*terpyridine monomer **73**, containing a flexible [18]crown-6 ether moiety, gave

the desired Archimedean-based cuboctahedron **74**; however, upon dilution or change of counterions, **74** underwent a quantitative transformation into two identical octahedrons **75**. Upon further dilution, four novel superposed *bis*triangular complexes **76** were generated (Figure 29).[165] These structures show a dynamic equilibrium simply by altering concentration or counterions; thus, upon concentration, **76** regenerated **75**, which with further concentration, **74** was isolated.

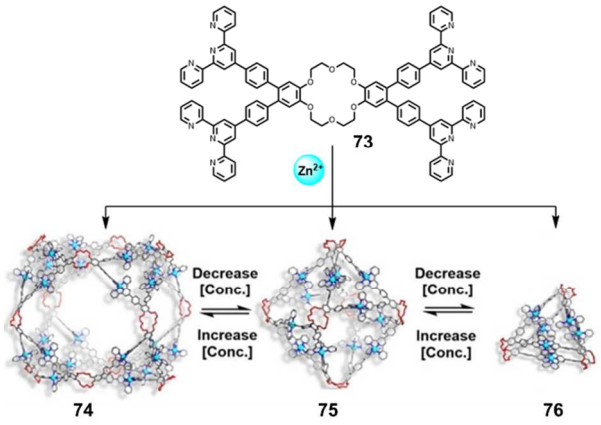


**Figure 29.** Self-assembly and controlled interconversion of crown ether functionalized cuboctahedron, octahedron and superposed-*bis*triangle cages. Adapted with permission from *J. Am. Chem. Soc.*, 2016, **138**, 12344-12347 (Copyright 2016 American Chemical Society).

Notably, in all of the above examples of molecular fission-fusion, there is no NMR or ESI-MS evidence for any intermediates during these interconversions. The key question is: how does one molecule transforms into exactly two equivalents of smaller discrete aggregates without forming any stable intermediate species? To probe the breadth of this novel quantitative interconversion, a new class of shape-persistent, three-dimensional $C_{3v}$-symmetric triptycene-based *tris*-terpyridinyl ligand (**77**) possessing shorter terpyridine arms was designed. The quantitative self-assembly of monomer **77** with $Zn^{2+}$ in 2:3 ratio initially gives a Platonic-based cubic architecture **78**, which was unequivocally characterized by single crystal X-ray structure analysis (Figure 30). The unique binding properties of the $Cd^{2+}$ analogue of this construct gave rise to a concentration-dependent dynamic equilibrium. Dilution transforms this cubic structure **79** into two identical tetrahedron-shaped complexes **81**, through a stable prism-shaped intermediate cage **80**. Unlike the previously reported system, here the structural conversions take place *via* a stable intermediate, which only exists in solution as a mixture with both or one of the terminal conformers, as determined by NMR.[166]

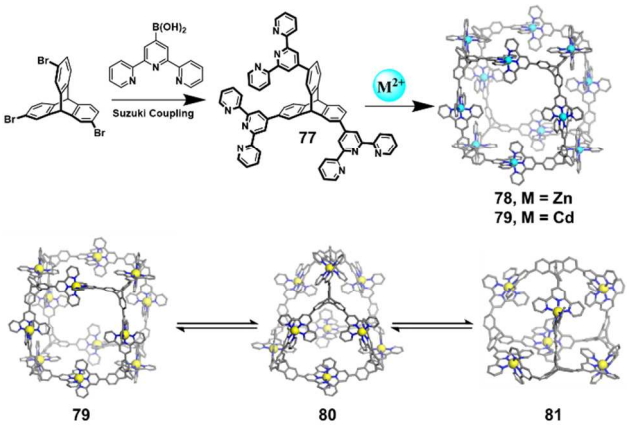


**Figure 30.** Concentration dependent reversible interconversion between a triptycene-based metallosupramolecular cube and tetrahedron through an intermediate prismatic cage. Reproduced with permission from *Dalton Trans.*, 2018, DOI:10.1039/C7DT04571A (Copyright 2018 The Royal Society of Chemistry).

A giant surface fluorinated metallodendritic supramolecular cage **83** with cuboctahedral core was created from the X-type building block **82** possessing a triangle connected by three <tpy-$Ru^{2+}$-tpy> linkages upon treatment with the exact ratio of $Zn^{2+}$ (Figure 31). Interestingly, the replacement of $Zn^{2+}$ with $Cd^{2+}$ leads to the generation of a smaller octahedral dendritic cage **84**.[167] Concentration changes for **83** and **84** do not exhibit a transition to another conformer; whereas, a similar metallodendritic cage decorated with long docosyl chains instead of fluorine,[168] again revealed the concentration-dependent interconversion between the cuboctahedron and octahedron core. This fission-fusion process was supported by TEM imaging. The high-yield generation of a branched nanostructure possessing a dendritic framework introduced a novel method to design and construct structurally precise metallodendrimers *via* the construction of the internal core itself. This strategy also opened the routes to potential internal unimolecular micelles which have the unique ability to contract under dilute conditions.

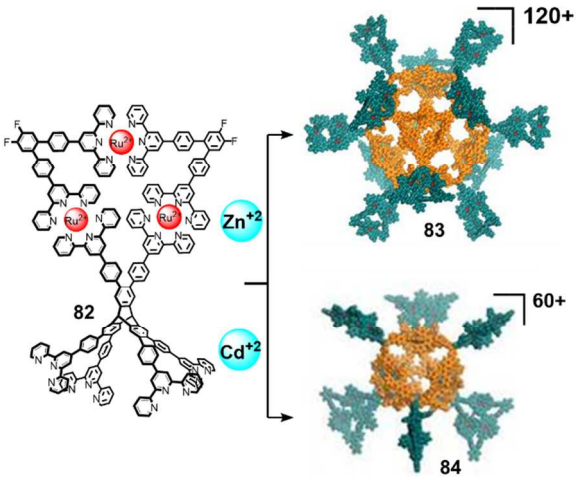


**Figure 31.** Self-assembly of supercharged metallodendrimers with cuboctahedron and octahedron core. Adapted with permission from *J. Am. Chem. Soc.*, 2017, **139**, 15652-15655 (Copyright 2017 American Chemical Society).

### 4.2. Component-induced supramolecular transformations

The majority of metallosupramolecular constructs utilize a homoleptic assembly involving symmetric monomers; however, heteroleptic assemblies involving multiple components have remained a challenge because of the self-sorting associated with structurally similar ligands and thermodynamically favored by-products.[169-171] Sometimes the addition of a new monomer that is architecturally different than original metallosupramolecules or a combination of different metallosupramolecular structures can lead to the disassembly and reassembly of the components, affording the generation of new discrete heteroleptic molecular artifacts.[161, 172-176] In such cases, more than one species can reshuffle from their initial state to only one final metallosupramolecular construct, which can contain all of the individual components.

The supramolecular transformation of novel terpyridine-based bimetallic triangles *via* the metallomacrocyclic rearrangement of a metallotriangle with a metallosquare was reported.[177] The 60°-*bis*terpyridine linker **5** and the $Ru^{2+}$-dimer **9** self-assembled to metallotriangle **85** and the metallosquare **86**, respectively.[153, 178] Mixing metallocyclic trimer **85** and tetramer **86** in precise 1:1.5 stoichiometry facilitated the quantitative generation of a new heteroleptic bimetallic-triangle **87** (Figure 32). This transformation of products to, in essence, other reagents opens new doorways to new heteronuclear products. As the self-sorting of ligand **5** and dimer **9** produced lesser number of species compared to their heteroleptic assembly producing **87**; the dynamic equilibria prefers the entropically favorable later process.

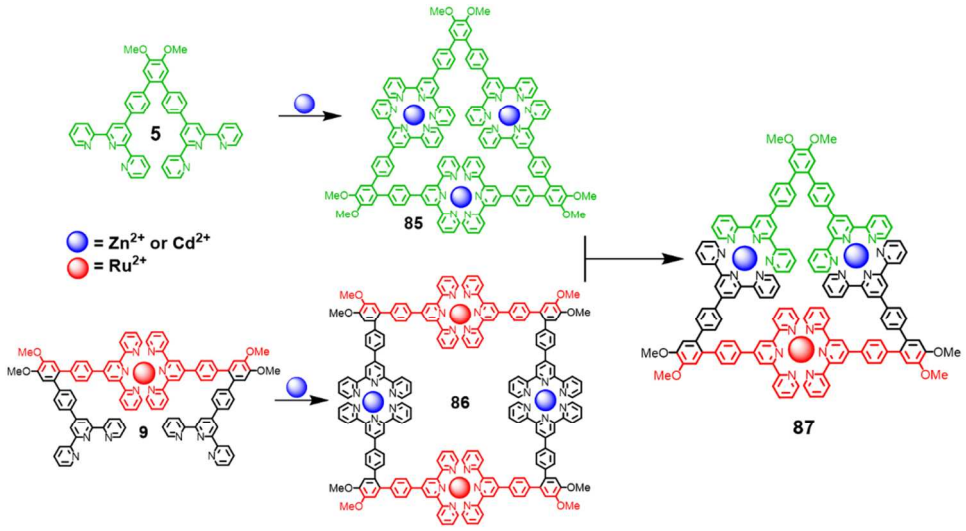


**Figure 32.** Quantitative rearrangement of triangle **85** and tetramer **86** to bimetallic heteroleptic triangle **87**. Adapted with permission from *Chem. Commun*., 2015, **51**, 12851-12864 (Copyright 2015 The Royal Society of Chemistry).

More recently another interesting molecular transformation from a 3D helix into a 2D rhomboidal structure was achieved by a precise component association.[179] A terpyridine-based 3D helical structure **89** was assembled by the treatment of *bis*$Ru^{2+}$-trimer **88** with $Zn^{2+}$ in a 2:3 stoichiometric ratio in MeCN. The possible structural rearrangement between helix **89** and *tris*terpyridine ligand **R3** to produce a more stable rhomboidal architecture was envisioned,

based on geometrical and topological analyses. Thus, the addition of ligand **R3** and $Zn^{2+}$ into a solution of helix **89** facilitated its quantitative transformation to the stable metallo-rhomboid **90** (Figure 33). Notably, again there is no NMR evidence for any acyclic intermediates during this transformation.

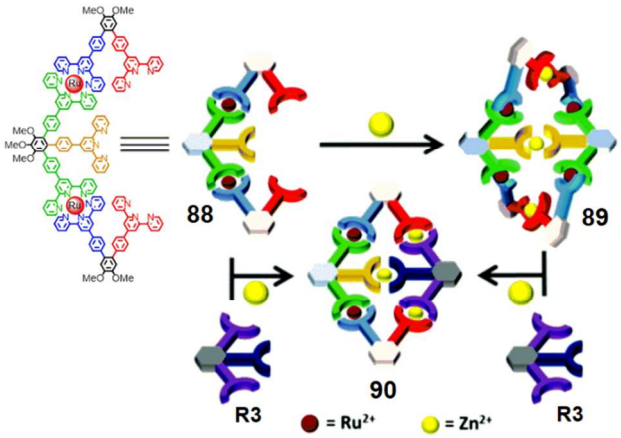


**Figure 33.** Self-assembly of 3D helix **89** and component-induced rearrangement to planar rhomboidal architecture **90**. Reproduced with permission from *Chem. Commun.*, 2016, **52**, 9773-9776 (Copyright 2016 The Royal Society of Chemistry).

### 4.3. Temperature-induced supramolecular transformations.

Coordination-driven self-assembly of metallosupramolecular architectures is a consequence of both kinetic and thermodynamic control, where the generation of final robust structures is the result of a one-sided directed equilibrium. Reversible metal-ligand coordination bonding provides an ideal platform in which to study such supramolecular transformations. Terpyridine-based monomers have the ability to coordinate diverse metal ions that facilitate both labile (M = $Zn^{2+}$, $Cd^{2+}$) and non-labile (M = $Fe^{2+}$, $Ru^{2+}$, $Os^{2+}$) <tpy-$M^{2+}$-tpy> connectivity. Thermodynamic control over the self-assembly process is essentially lost when non-labile metal ions are employed, since once the complex is formed it is irreversible and thus stable; whereas, kinetic control provides more stable thermodynamic products. The interconversion between kinetic and thermodynamic conformers is only possible under the influence of appropriate external stimuli, such as temperature. Because thermal energy is proportionally dependent on temperature; the thermodynamic conformer associated with a large energy barrier can sometimes be obtained at high temperature, whereas low temperature favors kinetic product.

A *bis*$Ru^{2+}$-trimer **91** was synthesized by combining the $RuCl_3$ adduct of a "V" type 60°-ligand and two 120°-*bis*terpyridine *via* a two-step synthetic procedure. The treatment of trimer **91** with $Fe^{2+}$ gave linear metallopolymer **92** at 25 °C but it can be converted to macrocycle **93** through a thermodynamic disassembly process by simply increasing reaction temperature (Figure 34).[180] Thus, the initial metallopolymer **92** is a kinetic intermediate, which can be transformed to the more stable hexanuclear metallocycle **93** *via* a thermodynamic disassembly/reassembly

process. The angular constraints, as shown above with the terpyridine-based Dondorff structures,[153] restrict the 2D planar conformation for the macrocycle and impose a 3D chair-like conformation.

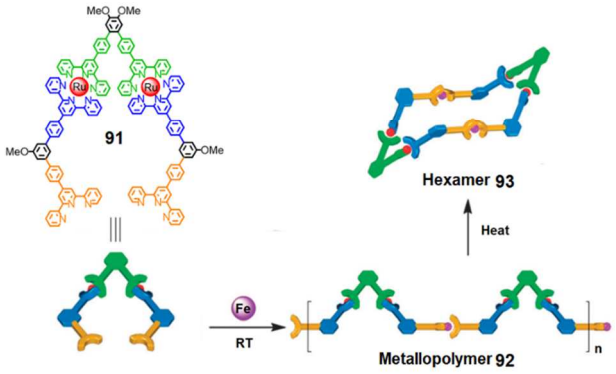


**Figure 34.** Thermodynamic conversion of metallopolymer **92** into hexameric metallocycle **93**. Adapted with permission from *Chem. Commun.*, 2015, **51**, 5766-5769 (Copyright 2015 The Royal Society of Chemistry).

Liu *et. al*. reported a similar thermal-responsive transformation of a metallopolymer to bimetallic metallo-triangle by combination of *bis*$Ru^{2+}$-trimer **94** and $Fe^{2+}$.[181] The trimer **94** was obtained by treatment of *bis*terpyridine **5** with $RuCl_3$; its subsequent reaction with $Fe^{2+}$ gave linear polymer **95**, which was quantitatively transformed to thermodynamically more stable triangle **96** at 80 °C (Figure 35). The site-to-site metallo-transformation of the $Zn^{2+}$ analogue (**97**) of the metallotriangle to **96** at 25 °C was found to be driven by low activation energies.

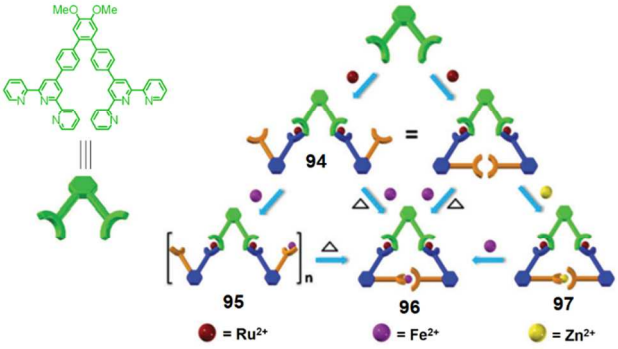


**Figure 35.** Pictorial illustration of temperature-induced conversion of metallopolymer **95** into discrete metallotriangle **96** and route of transmetalation from triangle **97** to **96**. Reproduced with permission from *Chem. Commun.*, 2016, **52**, 2513-2516 (Copyright 2016 The Royal Society of Chemistry).

Thus, when a flexible *tris*terpyridine ligand **98** with trigonal-*N* core was reacted with $Ru(DMSO)_4Cl_2$ in a 2:3 ratio, it generated in one-step the highly symmetrical 3D pseudo-octahedral complex **99**,[182] composed of four ligands and six $Ru^{2+}$ ion, in accordance with previously reported nanosphere construction using the related *tris*terpyridine monomer.[138] To introduce rigidity, **98** was dimerized to form the corresponding mono$Ru^{2+}$ complex **100**, which now possesses four terminal-free terpyridine moieties. The complexation between dimer **100** and $Fe^{2+}$ demonstrates an unexpected temperature-dependent assembly between two irreversible

isomeric 3D nanocages. At 25 °C, this complex gave nanocage **101**; while at 80° C, it generated another conformational isomer **102** (Figure 36). Thus, changes in reaction temperature can also play an important role in possible structural outcome and provides insight into the overall thermodynamic stability. This strategy of macromolecular assembly was further applied to creation of a similar 3D structure possessing three different metal centers ($Zn^{2+}$, $Ru^{2+}$, and $Fe^{2+}$) within a discrete molecular framework.[183] Relying on this design principle, the self-assembly of a series of tetrameric and hexameric macrocycles was exploited by using a similar *tris*dentate ligand with extended terpyridine arms.[184]

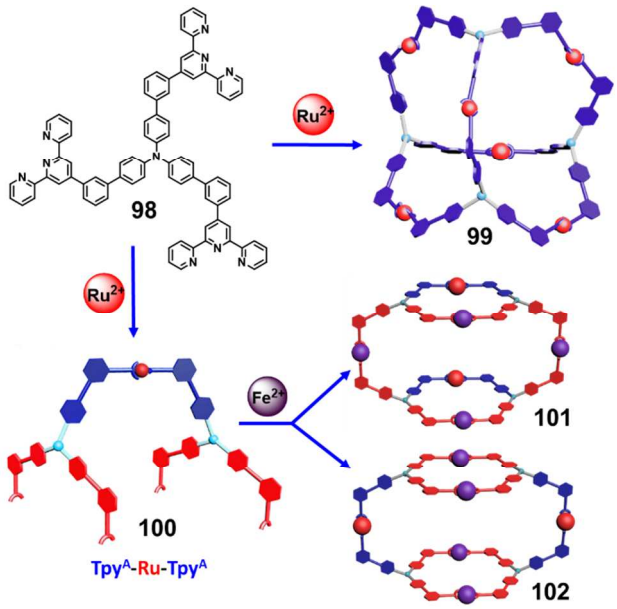


**Figure 36.** Synthesis of molecular nanosphere **99**. Temperature-dependent synthesis of irreversible, 3D, isomeric nanocages **101** and **102** from mono$Ru^{2+}$ terpyridinyl dimer **100**. Reproduced with permission from *J. Am. Chem. Soc.*, 2017, **139**, 3012-3020 (Copyright 2017 American Chemical Society).

## 5. Functional Nanomaterials

Inspiration originating from biological hierarchical self-assembly of polypeptides to secondary and tertiary ordered nanostructures using *H*-bonding and hydrophilic/hydrophobic interactions has paved the way to the design and construction of abiological nanomaterials capable of highly specific functionalities. Recently, fabrication of functional nanostructures with unprecedented structures and smart stimuli-responsive behavior is of special interest because of their potential biomedical applications, as drug delivery agents.[185-188] In view of their unique electrochemical, catalytic, and photophysical properties,[61] <tpy-$M^{2+}$-tpy> complexes were incorporated into a polymer backbone,[189, 190] and functionalized with nanoparticles,[81] carbon nanotubes,[191-193] and surfaces[79] to develop potentially utilitarian nanomaterials. These terpyridine-based materials were used to explore their potential for biomedical applications[61, 96] and optoelectronic devices.[61, 194] More recent research efforts have been focused on the hierarchical self-assembly of functionalized discrete metallomacrocycles for the construction of large-scale highly ordered organometallic nanostructures utilizing orthogonal metal-ligand coordination bonds and other non-covalent interactions.[26] Upon equilibrium between the

aggregated and non-aggregated states, these materials exhibit many interesting properties, such as: self-healing, recyclability, and high sensitivity to external stimuli.[195]

The research group of Stang and Yang has reported the synthesis of new amphiphilic rhomboidal and hexagonal Pt(II)/Pd(II)-macrocycles and explored their assembly into highly ordered nanostructures and supramolecular polymer gels.[14, 196-198] In the arena of terpyridine-based metallomacrocycles, the previous approaches have primarily focused on ion pairing.[199] The self-assembly of structurally rigid C6-functionalized, $Ru^{2+}$-hexameric macrocycles (possessing 12+ charge) with dodecacarboxylate-coated polyanionic dendrimers ($12^{-}$ charge) through electrostatic interaction was explored. The spontaneous hierarchical formation of a dendrimer-macrocycle composite in the form of nanofibers was revealed by TEM imaging. This result demonstrates the potential to employ polyanionic architectures in contrast to traditional monoionic counterions, as aids in shape-control for the exploration of new materials. With the need to explore the utility of the metallotriangles to self-assemble into ordered ion paired arrays, a series of $Zn^{2+}$ and $Cd^{2+}$ triangular materials were synthesized.[178] The pairing of hexavalent positively charged metallotriangles **103** with benzenehexacarboxylate afforded ion-paired nanofibers using a mixed solvent system, prepared from dilute solutions (~1 mM) of metallocycle in MeCN and sodium benzenehexacarboxylate in water (Figure 37). TEM images revealed large bundled structures with diameters *ca* 300 nm comprised of smaller organized fibers with diameters *ca*. 20 nm closely corresponding to the triangular side length. Based on PXRD and SAXD data, the molecular packing of triangles in the fiber was proposed using computer generated molecular modeling.

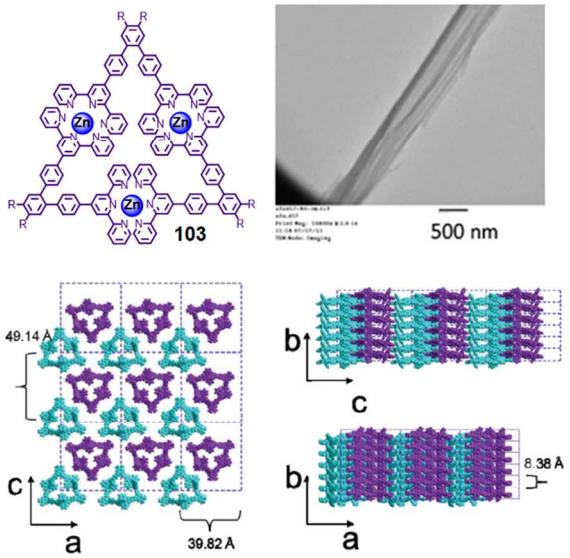


**Figure 37.** TEM image of fiber formed from triangle with benzenehexacarboxylate using ion pairing approach. Proposed packing model of triangles in fiber. Adapted with permission from *Dalton Trans.*, 2012, **41**, 11573-11575 (Copyright 2012 The Royal Society of Chemistry).

In both cases, the resultant nanocomposite fibers, obtained by using an electrostatic pairing strategy, were reported to be insoluble, potentially limiting some of the advantages of supramolecular functional materials. However, when a modified sugar-containing 120°-

*bis*terpyridine ligand was treated with $Fe^{2+}$, the predesigned peripherally functionalized hexameric construct was realized along with uniquely constrained pentameric macrocycle.[200] The self-assembled nanofibers of both the rings were generated by slowly diffusing hexane into a homogeneous solution of macrocycles. In each case, fibrous assemblies with the lengths of several micrometers in which most fibers possess diameters of 20–30 nm. More recently, a series of amphiphilic <tpy-$M^{2+}$-tpy> triangular macrocycles was evaluated.[201] The C16-long alkylated metallotriangles (**105**) were synthesized from ligand **104** and fully characterized (Figure 38). The secondary assembly of these metallotriangles into ordered nanostructures was studied by TEM imaging to gauge the e□ects of molecular topology, solvent, counterion, and metal center(s) on morphology and nanocomposition. The formation of highly directional lamellar and rod-like structures with sharp, uniform edges was observed with both the labile ($Zn^{2+}$) and non-labile ($Fe^{2+}$) systems. Molecular modelling, based on electron di□raction (SAXD) studies, indicated the presence of intermolecular π–π stacking between amphiphilic metallotriangles. E□ects of counterion and solvent were studied with the non-labile system. Depending on solvent conditions, counter ions have an impact on the aggregated morphology giving either disordered lamellae or nanotubes. In this study, the amphiphilicity provides a mechanism for enhanced ordering relative to nonamphiphilic controls.

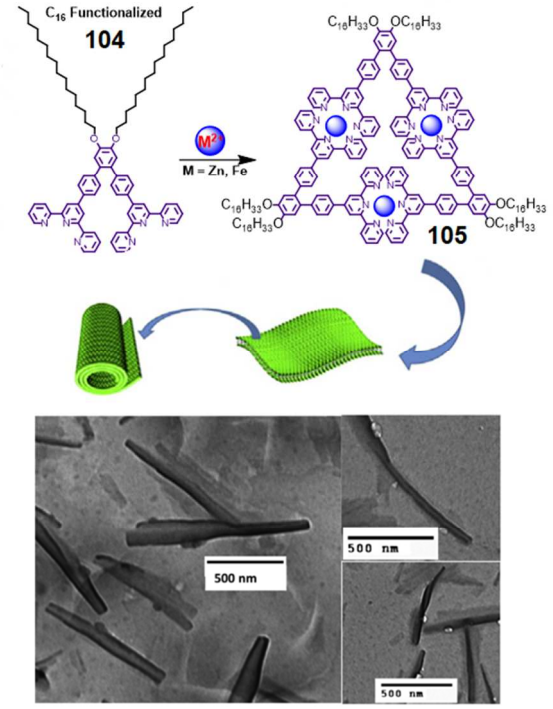


**Figure 38.** Self-assembly of the *bis*-C16 functionalized amphiphilic metallotriangles **105** and illustration of their subsequent hierarchical ordering into nanostructures. TEM images of **105** ordered into tube-like structure. Adapted with permission from *Supramol. Chem.*, 2017, **29**, 69-79 (Copyright 2017 Taylor & Francis). Graphics adapted with permission from lee and coworkers, *Acc. Chem. Res.*, 2011, 44, 72–82 (copyright 2011 American Chemical Society).

## 6. Conclusion

Recent advances in terpyridine-based metallosupramolecular architectures are dominated by complex and multifunctional higher-order structural design. Diverse themes for designing of interesting fractal geometries are evolving with the use of increasing number of triangular frameworks as well as hexagonal fractals. More emphasis has been focused on the synthesis of novel 3D cages utilizing unique designer strategies involving *meta*-substitution, multiplanar vertices as well as flexible multitopic vertices. Step-wise synthetic protocols have been devised for the synthesis of heterometallic assemblies. Eliminating the possibility of planar geometry using pre-coordinated metal-organic ligands and utilizing step-wise synthetic protocol, the construction of several complex 3D-assemblies as well as metallodendrimers has been achieved. The incorporation of physiochemically important organic scaffolds into donor monomers resulted in interesting functional metallosupramolecules, in which these moieties can be an integral part of rigid directional vertices or attached as pendant, purposeful groups. The second order assembly of functional supramolecules further leads to more complex structural design(s). The hierarchical self-assembly strategy involving coordination bonding in conjugation with other non-covalent interactions has paved the way to generate ordered terpyridine-based supramolecular smart materials. There is increasing emphases on supramolecular interconversion between discrete terpyridine-based supramacromolecules triggered by the external stimuli, such as changing concentration, temperature, and/or counterions. The design of complicated dynamic supramacromolecular transformation systems generates specific outputs, such as tailored properties and functions. The inherent void regions and surface openings in these macromolecular cages, as well as the use of these architectural transformations, can be envisioned to lead to new avenues of molecular encapsulation and release.

## Acknowledgements

GRN would like to thank the numerous colleagues, who have assisted and contributed to this growing terpyridine-based fractal project over the years and are acknowledged on/in our publications. Support is also acknowledged from the National Science Foundation as well as James and Vanita Oelschlager funding *via* the University of Akron.

## References

1. C. J. Pedersen, *J. Am. Chem. Soc.*, 1967, **89**, 7017-7036.
2. J.-M. Lehn, *Pure Appl. Chem.*, 1978, **50**, 871-892.
3. D. J. Cram, *Angew. Chem. Int. Ed.*, 1988, **27**, 1009-1020.
4. D. J. Cram and J. M. Cram, *Science*, 1974, **183**, 803-809.
5. J. W. Steed and J. L. Atwood, *Supramolecular Chemistry*, John Wiley & Sons, Ltd, Chichester, England, 2000.
6. J. W. Steed, D. R. Turner and K. J. Wallace, *Core Concepts in Supramolecular Chemistry and Nanochemistry*, John Wiley & Sons Ltd., 2007.
7. T. R. Cook, V. Vajpayee, M. H. Lee, P. J. Stang and K.-W. Chi, *Acc. Chem. Res.*, 2013, **46**, 2464-2474.
8. M. L. Saha, X. Yan and P. J. Stang, *Acc. Chem. Res.*, 2016, **49**, 2527-2539.
9. C. J. Brown, F. D. Toste, R. G. Bergman and K. N. Raymond, *Chem. Rev.*, 2015, **115**, 3012-3035.

10. M. Raynal, P. Ballester, A. Vidal-Ferran and P. W. van Leeuwen, *Chem. Soc. Rev.*, 2014, **43**, 1734-1787.
11. M. Yoshizawa, J. K. Klosterman and M. Fujita, *Angew. Chem. Int. Ed.*, 2009, **48**, 3418-3438.
12. A. Coskun, J. M. Spruell, G. Barin, W. R. Dichtel, A. H. Flood, Y. Y. Botros and J. F. Stoddart, *Chem. Soc. Rev.*, 2012, **41**, 4827-4859.
13. D. B. Amabilino, D. K. Smith and J. W. Steed, *Chem. Soc. Rev.*, 2017, **46**, 2404-2420.
14. L.-J. Chen, G.-Z. Zhao, B. Jiang, B. Sun, M. Wang, L. Xu, J. He, Z. Abliz, H. Tan, X. Li and H.-B. Yang, *J. Am. Chem. Soc.*, 2014, **136**, 5993-6001.
15. B. Therrien, in *Chemistry of Nanocontainers*, eds. M. Albrecht and E. Hahn, Springer Berlin Heidelberg, Berlin, Heidelberg, 2012, DOI: 10.1007/128_2011_272, pp. 35-55.
16. P. Mukherjee, S. Pramanik and S. Shanmugaraju, in *Molecular Self-Assembly*, Pan Stanford Publishing, 2012, pp. 259-299.
17. S. Bhowmick, S. Chakraborty, A. Das, S. Nallapeta and N. Das, *Inorg. Chem.*, 2015, **54**, 8994-9001.
18. J.-M. Lehn, *Supramolecular Chemistry: Concepts and Perspectives*, VCH, Weinheim, 1995.
19. J. M. Lehn, *Angew. Chem. Int. Ed.*, 2013, **52**, 2836-2850.
20. J.-P. Sauvage, *Chem. Commun.*, 2005, 1507-1510.
21. F. Durola, V. Heitz, F. Reviriego, C. Roche, J.-P. Sauvage, A. Sour and Y. Trolez, *Acc. Chem. Res.*, 2014, **47**, 633-645.
22. J. P. Sauvage, *Angew. Chem. Int. Ed.*, 2017, **56**, 11080-11093.
23. J. F. Stoddart, *Chem. Soc. Rev.*, 2009, **38**, 1802-1820.
24. J. F. Stoddart, *Angew. Chem. Int. Ed.*, 2017, **56**, 11094-11125.
25. R. Chakrabarty, P. S. Mukherjee and P. J. Stang, *Chem. Rev.*, 2011, **111**, 6810-6918.
26. T. R. Cook and P. J. Stang, *Chem. Rev.*, 2015, **115**, 7001-7045.
27. K. Harris, D. Fujita and M. Fujita, *Chem. Commun.*, 2013, **49**, 6703-6712.
28. D. Fujita, Y. Ueda, S. Sato, N. Mizuno, T. Kumasaka and M. Fujita, *Nature*, 2016, **540**, 563-566.
29. G. R. Newkome and C. N. Moorefield, *Chem. Soc. Rev.*, 2015, **44**, 3954-3967.
30. J. M. Ludlow III and G. R. Newkome, in *Adv. Heterocycl. Chem.*, eds. E. F. V. Scriven and C. A. Ramsden, Elsvier Publishing, 2016, pp. 195-236.
31. S. De, K. Mahata and M. Schmittel, *Chem. Soc. Rev.*, 2010, **39**, 1555-1575.
32. M. L. Saha, S. Neogi and M. Schmittel, *Dalton Trans.*, 2014, **43**, 3815-3834.
33. M. Frank, M. D. Johnstone and G. H. Clever, *Chem. Eur. J.*, 2016, **22**, 14104-14125.
34. A. J. McConnell, C. S. Wood, P. P. Neelakandan and J. R. Nitschke, *Chem. Rev.*, 2015, **115**, 7729-7793.
35. L. J. Chen, H.-B. Yang and M. Shionoya, *Chem. Soc. Rev.*, 2017, **46**, 2555-2576.
36. S. Mukherjee and P. S. Mukherjee, *Chem. Commun.*, 2014, **50**, 2239-2248.
37. M. J. Wiester, P. A. Ulmann and C. A. Mirkin, *Angew. Chem. Int. Ed.*, 2011, **50**, 114-137.
38. D. A. Roberts, B. S. Pilgrim and J. R. Nitschke, *Chem. Soc. Rev.*, 2017, DOI: 10.1039/c6cs00907g.
39. G. H. Clever and P. Punt, *Acc. Chem. Res.*, 2017, **50**, 2233-2243.
40. N. J. Young and B. P. Hay, *Chem. Commun.*, 2013, **49**, 1354-1379.
41. R. S. Forgan, J.-P. Sauvage and J. F. Stoddart, *Chem. Rev.*, 2011, **111**, 5434-5464.
42. W. Weng, Y.-X. Wang and H.-B. Yang, *Chem. Soc. Rev.*, 2016, **45**, 2656-2693.
43. R. A. Bilbeisi, J.-C. Olsen, L. J. Charbonnière and A. Trabolsi, *Inorg. Chim. Acta*, 2014, **417**, 79-108.
44. N. B. Debata, D. Tripathy and D. K. Chand, *Coord. Chem. Rev.*, 2012, **256**, 1831-1945.
45. S. Kassem, T. van Leeuwen, A. S. Lubbe, M. R. Wilson, B. L. Feringa and D. A. Leigh, *Chem. Soc. Rev.*, 2017, **46**, 2592-2621.
46. S. Erbas-Cakmak, D. A. Leigh, C. T. McTernan and A. L. Nussbaumer, *Chem. Rev.*, 2015, **115**, 10081-10206.

47. S. Chakraborty, S. Mondal, S. Bhowmick, J. Ma, H. Tan, S. Neogi and N. Das, *Dalton Trans.*, 2014, **43**, 13270-13277.
48. S. Chakraborty, S. Mondal, Q. Li and N. Das, *Tetrahedron Lett.*, 2013, **54**, 1681-1685.
49. J. L. Greenfield, F. J. Rizzuto, I. Goldberga and J. R. Nitschke, *Angew. Chem. Int. Ed.*, 2017, **56**, 7541-7545.
50. J. M. Ludlow III, Z. Guo, A. Schultz, R. Sarkar, C. N. Moorefield, C. Wesdemiotis and G. R. Newkome, *Eur. J. Inorg. Chem.*, 2015, 5662-5669.
51. J.-L. Wang, X. Li, C. D. Shreiner, X. Lu, C. N. Moorefield, S. R. Tummalapalli, D. A. Medvetz, M. J. Panzner, F. R. Fronczek, C. Wesdemiotis and G. R. Newkome, *New J. Chem.*, 2012, **36**.
52. E. C. Constable, A. M. W. C. Thompson, P. Harveson, L. Macko and M. Zehnder, *Chem. Eur. J.*, 1995, **1**, 360-367.
53. M. Osawa, M. Hoshino, S. Horiuchi and Y. Wakatsuki, *Organometallics*, 1999, **18**, 112-114.
54. E. C. Constable, C. E. Housecroft, M. Cattalini and D. Phillips, *New J. Chem.*, 1998, **22**, 193-200.
55. G. S. Hanan, C. R. Arana, J.-M. Lehn and D. Fenske, *Angew. Chem. Int. Ed.*, 1995, **34**, 1122-1124.
56. G. S. Hanan, U. S. Schubert, D. Volkmer, E. Rivière, J.-M. Lehn, N. Kyritsakas and J. Fischer, *Can. J. Chem.*, 1997, **75**, 169-182.
57. D. M. Bassani, J.-M. Lehn, K. Fromm and D. Fenske, *Angew. Chem. Int. Ed.*, 1998, **37**, 2364-2367.
58. M. Barboiu, G. Vaughan, R. Graff and J.-M. Lehn, *J. Am. Chem. Soc.*, 2003, **125**, 10257-10265.
59. D. M. Bassani, J.-M. Lehn, S. Serroni, F. Puntoriero and S. Campagna, *Chem. Eur. J.*, 2003, **9**, 5936-5946.
60. G. R. Newkome, C. N. Moorefield and S. Chakraborty, *J. Inorg. Organomet. Polym. Mater.*, 2018, **28**, 360-368.
61. U. S. Schubert, A. Winter and G. R. Newkome, *Terpyridine-based Materials-For Catalytic, Optoelectronic, and Life Science Applications*, Wiley-VCH, Weinheim, 2011.
62. A. Winter and U. S. Schubert, *Chem. Soc. Rev.*, 2016, **45**, 5311-5357.
63. E. C. Constable, C. E. Housecroft, M. Neuburger, J. Schönle and J. A. Zampese, *Dalton Trans.*, 2014, **43**, 7227-7235.
64. C. E. Housecroft and E. C. Constable, *J. Inorg. Organomet. Polym. Mater.*, 2018, **28**, 414–427.
65. Y. Gao, D. Rajwar and A. C. Grimsdale, *Macromol. Rapid Commun.*, 2014, **35**, 1727-1740.
66. Z. Zheng, L. Opilik, F. Schiffmann, W. Liu, G. Bergamini, P. Ceroni, L.-T. Lee, A. Schütz, J. Sakamoto, R. Zenobi, J. VandeVondele and A. D. Schlüter, *J. Am. Chem. Soc.*, 2014, **136**, 6103-6110.
67. A. Fermi, G. Bergamini, M. Roy, M. Gingras and P. Ceroni, *J. Am. Chem. Soc.*, 2014, **137**, 6395-6400.
68. H. Maeda, R. Sakamoto and H. Nishihara, *Coord. Chem. Rev.*, 2017, **346**, 139-149.
69. M. L. Saha, K. Mahata, D. Samanta, V. Kalsani, J. Fan, J. W. Bats and M. Schmittel, *Dalton Trans.*, 2013, **42**, 12840-12843.
70. M. Schmittel, B. He and P. Mal, *Org. Lett.*, 2008, **10**, 2513-2516.
71. B. Champin, V. Sartor and J.-P. Sauvage, *New J. Chem.*, 2008, **32**, 1048-1054.
72. E. Coronado, J. R. Galan-Mascaros, P. Gaviña, C. Martí-Gastaldo, F. M. Romero and S. Tatay, *Inorg. Chem.*, 2008, **47**, 5197-5203.
73. S. Ghosh, G. T. Silber, A. J. P. White, N. Robertson and R. Vilar, *Dalton Trans.*, 2013, **42**, 13813-13816.
74. R. Trokowski, S. Akine and T. Nabeshima, *Chem. Commun.*, 2008, 889-890.
75. R. Trokowski, S. Akine and T. Nabeshima, *Chem. Eur. J.*, 2011, **17**, 14420-14428.
76. S. Perera, X. Li, M. Soler, A. Schlutz, C. Wesdemiotis, C. N. Moorefield and G. R. Newkome, *Angew. Chem. Int. Ed.*, 2010, **49**, 6539-6544.

77. S. Perera, X. Li, M. Soler, C. Wesdemiotis, C. N. Moorefield and G. R. Newkome, *Chem. Commun.*, 2011, **47**, 4658-4660.
78. B. Laramee-Milette, C. Lachance-Brais and G. S. Hanan, *Dalton Trans.*, 2015, **44**, 41-45.
79. A. Winter, S. Hoeppener, G. R. Newkome and U. S. Schubert, *Adv. Mater.*, 2011, **23**, 3484-3498.
80. A. Winter, G. R. Newkome and U. S. Schubert, *ChemCatChem*, 2011, **3**, 1384-1406.
81. A. Winter, M. D. Hager, G. R. Newkome and U. S. Schubert, *Adv. Mater.*, 2011, **23**, 5728-5748.
82. H.-J. Schneider, *Angew. Chem. Int. Ed*, 2009, **48**, 3924-3977.
83. S. Loffler, A. Wuttke, B. Zhang, J. J. Holstein, R. A. Mata and G. H. Clever, *Chem.Commun.*, 2017, **53**, 11933-11936.
84. A. Juris, V. Balzani, F. Barigelletti, S. Campagna, P. Belser and A. von Zelewsky, *Coord. Chem. Rev*, 1988, **84**, 85-277.
85. V. Balzani and A. Juris, *Coord. Chem. Rev*, 2001, **211**, 97-115.
86. C. Tan, S. Yang, N. R. Champness, X. Lin, A. J. Blake, W. Lewis and M. Schröder, *Chem. Commun*, 2011, **47**, 4487-4489.
87. D. Maity, S. Das, S. Mardanya and S. Baitalik, *Inorg. Chem.*, 2014, **52**, 6820-6838.
88. R. Alberto, G. Bergamaschi, H. Braband, T. Fox and V. Amendola, *Angew. Chem. Int. Ed.*, 2012, **51**, 9772 - 9776.
89. P. Howlader, P. Das, E. Zangrando and P. S. Mukherjee, *J. Am. Chem. Soc.*, 2016, **138**, 1668-1676.
90. D. Preston, A. Fox-Charles, W. K. C. Lo and J. D. Crowley, *Chem. Commun*, 2015, **51**, 9042-9045.
91. C. A. Nijhuis, B. J. Ravoo, J. Huskens and D. N. Reinhoudt, *Coord. Chem. Rev.*, 2007, **251**, 1761-1780.
92. S. Cerfontaine, L. Marcelis, B. Laramee-Milette, G. S. Hanan, F. Loiseau, J. De Winter, P. Gerbaux and B. Elias, *Inorg. Chem.*, 2018, **57**, 2639-2653.
93. A. K. Pal, B. Laramée-Milette and G. S. Hanan, *Inorg. Chim. Acta*, 2014, **418**, 15-22.
94. A. K. Pal and G. S. Hanan, *Chem Soc. Rev.*, 2014, **43**, 6184-6197.
95. I. Eryazici, C. N. Moorefield and G. R. Newkome, *Chem. Rev.*, 2008, **108**, 1834-1895.
96. A. Winter, M. Gottschaldt, G. R. Newkome and U. S. Schubert, *Curr. Top. Med. Chem.*, 2012, **12**, 158-175.
97. K. Karidi, A. Garoufis, N. Hadjichristidis and J. Reedijk, *Dalton Trans.*, 2005, 728-734.
98. K. Karidi, A. Garoufis, A. Tsipis, N. Hadjiliadis, H. den Dulk and J. Reedijk, *Dalton Trans.*, 2005, 1176-1187.
99. G. R. Newkome, T. J. Cho, C. N. Moorefield, G. R. Baker, M. J. Saunders, R. Cush and P. S. Russo, *Angew. Chem. Int. Ed.*, 1999, **38**, 3717-3721.
100. G. R. Newkome, P. Wang, C. N. Moorefield, T. J. Cho, P. Mohapatra, S. Li, S.-H. Hwang, O. Lukoyanova, L. Echegoyen, J. A. Palagallo, V. Iancu and S.-W. Hla, *Science*, 2006, **312**, 1782-1785.
101. J.-L. Wang, X. Li, X. Lu, I.-F. Hsieh, Y. Cao, C. N. Moorefield, C. Wesdemiotis, S. Z. D. Cheng and G. R. Newkome, *J. Am. Chem. Soc.*, 2011, **133**, 11450-11453.
102. X. Lu, X. Li, J.-L. Wang, C. N. Moorefield, C. Wesdemiotis and G. R. Newkome, *Chem. Commun.*, 2012, **48**, 9873-9875.
103. A. Schultz, X. Li, B. Barkakaty, C. N. Moorefield, C. Wesdemiotis and G. R. Newkome, *J. Am. Chem. Soc.*, 2012, **134**, 7672-7675.
104. R. Sarkar, K. Guo, C. N. Moorefield, M. J. Saunders, C. Wesdemiotis and G. R. Newkome, *Angew. Chem. Int. Ed.*, 2014, **53**, 12182-12185.
105. S. Chakraborty, R. Sarkar, K. Endres, T.-Z. Xie, M. Ghosh, C. N. Moorefield, C. Wesdemiotis and G. R. Newkome, *Eur. J. Org. Chem.*, 2016, 5091-5095.
106. Z. Jiang, Y. Li, M. Wang, D. Liu, J. Yuan, M. Chen, J. Wang, G. R. Newkome, W. Sun, X. Li and P. Wang, *Angew. Chem. Int. Ed.*, 2017, **56**, 11450-11455.

107. Y. Li, Z. Jiang, M. Wang, J. Yuan, D. Liu, X. Yang, M. Chen, J. Yan, X. Li and P. Wang, *J. Am. Chem. Soc.*, 2016, **138**, 10041-10046.
108. Z. Jiang, Y. Li, M. Wang, B. Song, K. Wang, M. Sun, D. Liu, X. Li, J. Yuan, M. Chen, Y. Guo, X. Yang, T. Zhang, C. N. Moorefield, G. R. Newkome, B. Xu, X. Li and P. Wang, *Nat. Commun.*, 2017, **8**, doi: 10.1038/ncomms15476.
109. Z. Zhang, H. Wang, X. Wang, Y. Li, B. Song, O. Bolarinwa, R. A. Reese, T. Zhang, X.-Q. Wang, J. Cai, B. Xu, M. Wang, C. Liu, H.-B. Yang and X. Li, *J. Am. Chem. Soc.*, 2017, **139**, 8174–8185.
110. M. Wang, C. Wang, X.-Q. Hao, J. Liu, X. Li, C. Xu, A. Lopwz, L. Sun, M.-P. Song, H.-B. Yang and X. Li, *J. Am. Chem. Soc.*, 2014, **136**, 6664-6671.
111. Y.-T. Chan, X. Li, C. N. Moorefield, C. Wesdemiotis and G. R. Newkome, *Chem. Eur. J.*, 2011, **17**, 7750-7754.
112. Y.-T. Chan, X. Li, J. Yu, G. A. Carri, C. N. Moorefield, C. Wesdemiotis and G. R. Newkome, *J. Am. Chem. Soc.*, 2011, **133**, 11967-11976.
113. X. Li, Y.-T. Chan, M. Casiano-Maldonado, J. Yu, G. A. Carri, G. R. Newkome and C. Wesdemiotis, *Anal. Chem.*, 2011, **83**, 6667-6674.
114. T. Wu, J. Yuan, B. Song, Y. S. Chen, M. Chen, X. Xue, Q. Liu, J. Wang, Y.-T. Chan and P. Wang, *Chem. Commun.*, 2017, **53**, 6732-6735.
115. Y.-P. Liang, Y.-J. He, Y.-H. Lee and Y.-T. Chan, *Dalton Trans*, 2015, **44**, 5139-5145.
116. J. H. Fu, Y. H. Lee, Y. J. He and Y.-T. Chan, *Angew. Chem. Int. Ed.*, 2015, **54**, 6231-6235.
117. S. Y. Wang, J. H. Fu, Y. P. Liang, Y. J. He, Y. S. Chen and Y.-T. Chan, *J. Am. Chem. Soc.*, 2016, **138**, 3651-3654.
118. M. Wang, K. Wang, C. Wang, M. Huang, X. Q. Hao, M. Z. Shen, G. Q. Shi, Z. Zhang, B. Song, A. Cisneros, M. P. Song, B. Xu and X. Li, *J. Am. Chem. Soc.*, 2016, **138**, 9258-9268.
119. G.-Q. Yin, H. Wang, X.-Q. Wang, B. Song, L.-J. Chen, L. Wang, X.-Q. Hao, H.-B. Yang and X. Li, *Nat. Commun.*, 2018, **9**, doi:10.1038/s41467-41018-02959-w.
120. T.-Z. Xie, J.-Y. Li, Z. Guo, J. M. Ludlow III, X. Lu, C. N. Moorefield, C. Wesdemiotis and G. R. Newkome, *Eur. J. Inorg. Chem.*, 2016, 1671-1677.
121. Y. M. Klein, A. Prescimone, E. C. Constable and C. E. Housecroft, *CrystEngComm*, 2015, **17**, 6483-6492.
122. Y. M. Klein, A. Prescimone, M. B. Pitak, S. J.Coles, E. C. Constable and C. E. Housecroft, *CrystEngComm*, 2016, **18**, 4704-4707.
123. S. Vojovic, E. C. Constable, C. E. Housecroft, C. D. Morris, M. Neuburger and A. Prescimone, *Polyhedron*, 2015, **92**, 77-83.
124. S.-H. Hwang, P. Wang, C. N. Moorefield, L. A. Godínez, J. Manríquez, E. Bustos and G. R. Newkome, *Chem. Commun.*, 2005, 4672-4674.
125. Y. Gao, T. He, P. Hu, T. M. Koh, H. Sun and A. C. Grimsdale, *Macromol. Chem. Phys.*, 2014, **215**, 753-762.
126. J. K. Klosterman, J. Veliks, D. K. Frantz, Y. Yasui, M. Loepfe, E. Zysman-Colman, A. Linden and J. S. Siegel, *Org. Chem. Front.*, 2016, **3**, 661-666.
127. J. Veliks, H. M. Seifert, D. K. Frantz, J. K. Klosterman, J.-C. Tseng, A. Linden and J. S. Siegel, *Org. Chem. Front.*, 2016, **3**, 667-672.
128. M. Yamamura, K. Yamakawa, Y. Okazaki and T. Nabeshima, *Chem. Eur. J.*, 2014, **20**, 16258-16265.
129. Y. Yao, S. Chakraborty, S. Zhu, K. J. Endres, T. Z. Xie, W. Hong, E. Manandhar, C. N. Moorefield, C. Wesdemiotis and G. R. Newkome, *Chem. Commun.*, 2017, **53**, 8038-8041.
130. A. K. Pal, B. Laramée-Milette and G. S. Hanan, *RSC Advances*, 2014, **4**, 21262–21266.
131. J.-J. Liu, Y.-J. Lin and G.-X. Jin, *Organometallics*, 2014, **33**, 1283-1290.
132. H. Sepehrpour, M. L. Saha and P. J. Stang, *J. Am. Chem. Soc.*, 2017, **139**, 2553-2556.

133. G. Vernizzi and M. Olvera de la Cruz, *Proc. Natl. Acad. Sci.*, 2007, **104**, 18382-18386.
134. S. M. Stagg, C. Gürkan, D. M. Fowler, P. LaPointe, T. R. Foss, C. S. Potter, B. Carragher and W. E. Balch, *Nature*, 2006, **439**, 234-238.
135. T. Schröder, R. Brodbeck, M. C. Letzel, A. Mix, B. Shnatwinkel, M. Tonigold, D. Volkmer and J. Mattay, *Tetrahedron Lett.*, 2008, **49**, 5939-5942.
136. X. Lu, X. Li, Y. Cao, A. Schultz, J.-L. Wang, C. N. Moorefield, C. Wesdemiotis, S. Z. D. Cheng and G. R. Newkome, *Angew. Chem. Int. Ed.*, 2013, **52**, 7728-7731.
137. X. Lu, X. Li, K. Guo, J. Wang, M. Huang, J.-L. Wang, T.-Z. Xie, C. N. Moorefield, S. Z. D. Cheng, C. Wesdemiotis and G. R. Newkome, *Chem. Eur. J.*, 2014, **20**, 13094-13098.
138. T.-Z. Xie, S.-Y. Liao, K. Guo, X. Lu, X. Dong, M. Huang, C. N. Moorefield, S. Z. D. Cheng, X. Liu, C. Wesdemiotis and G. R. Newkome, *J. Am. Chem. Soc.*, 2014, **136**, 8165-8168.
139. M. Chen, J. Wang, D. Liu, Z. Jiang, Q. Liu, T. Wu, H. Liu, W. Yu, J. Yan and P. Wang, *J. Am. Chem. Soc.*, 2018, **140**, 2555-2561.
140. T.-Z. Xie, K. Guo, M. Huang, X. Lu, S.-Y. Liao, R. Sarkar, C. N. Moorefield, S. Z. D. Cheng, C. Wesdemiotis and G. R. Newkome, *Chem. Eur. J.*, 2014, **20**, 11291-11294.
141. C. Wang, X.-Q. Hao, M. Wang, C. Guo, B. Xu, E. N. Tan, Y.-Y. Zhang, Y. Yu, Z.-Y. Li, H.-B. Yang, M.-P. Song and X. Li, *Chem. Sci.*, 2014, **5**, 1221-1226.
142. M. Wang, C. Wang, X.-Q. Hao, X. Li, T. J. Vaughn, Y.-Y. Zhang, Y. Yu, Z.-Y. Li, M.-P. Song, H.-B. Yang and X. Li, *J. Am. Chem. Soc.*, 2014, **136**, 10499-10507.
143. T.-Z. Xie, K. Guo, Z. Guo, W.-Y. Gao, L. Wojtas, G.-H. Ning, M. Huang, X. Lu, J.-Y. Li, S.-Y. Liao, Y.-S. Chen, C. N. Moorefield, M. J. Saunders, S. Z. D. Cheng, C. Wesdemiotis and G. R. Newkome, *Angew. Chem. Int. Ed.*, 2015, **54**, 9224-9229.
144. E. C. Constable, C. E. Housecroft and C. B. Smith, *Inorg. Chem. Commun.*, 2003, **6**, 1011-1013.
145. E. C. Constable, C. E. Housecroft, M. Neuburger, S. Schaffner and C. B. Smith, *Dalton Trans.*, 2005, 2259-2267.
146. H. S. Chow, E. C. Constable, C. E. Housecroft, M. Neuberger and S. Schaffner, *Polyhedron*, 2006, **25**, 1831-1843.
147. P. R. Andres and U. S. Schubert, *Synthesis*, 2004, 1229-1238.
148. A. Ostrowicki, E. Koepp and F. Vögtle, *Top. Curr. Chem.*, 1991, **161**, 37-66.
149. G. R. Newkome, K. S. Yoo and C. N. Moorefield, *Chem. Commun.*, 2002, 2164-2165.
150. J. M. Ludlow III, T. Xie, Z. Guo, K. Guo, M. J. Saunders, C. N. Moorefield, C. Wesdemiotis and G. R. Newkome, *Chem. Commun.*, 2015, **51**, 3820-3823.
151. Y.-C. Wang, Y.-P. Liang, J.-Y. Cai, Y.-J. He, Y.-H. Lee and Y.-T. Chan, *Chem. Commun.*, 2016, **52**, 12622-12625.
152. T.-Z. Xie, K. Guo, J.-Y. Li, B. Zhang, K. Zheng, C. N. Moorefield, M. J. Saunders, K. J. Endres, S. Sallam, C. Wesdemiotis and G. R. Newkome, *J. Inorg. Organomet. Polym. Mater.*, 2016, **26**, 907-913.
153. A. Schultz, X. Li, J. K. McCusker, C. N. Moorefield, F. N. Castellano, C. Wesdemiotis and G. R. Newkome, *Chem. Eur. J.*, 2012, **18**, 11569-11572.
154. A. Schultz, X. Li, C. N. Moorefield, C. Wesdemiotis and G. R. Newkome, *Eur. J. Inorg. Chem.*, 2013, 2492-2497.
155. J. Yang, M. Bhadbhade, W. A. Donald, H. Iranmanesh, E. G. Moore, H. Yan and J. E. Beves, *Chem. Commun.*, 2015, **51**, 4465-4468.
156. C. Shen, A. D. W. Kennedy, W. A. Donald, A. M. Torres, W. S. Price and J. E. Beves, *Inorg. Chim. Acta*, 2017, **458**, 122-128.
157. S. Gaikwad, M. Lal Saha, D. Samanta and M. Schmittel, *Chem. Commun.*, 2017, **53**, 8034-8037.
158. T. W. Bell and H. Jousselin, *Nature*, 1994, **367**, 441-444.

159. S. M. Stagg, P. LaPointe, A. Razvi, C. Gurkan, C. S. Potter, B. Carragher and W. E. Balch, *Cell*, 2008, **134**, 474-484.
160. K. A. Dill and J. L. MacCallum, *Science*, 2012, **338**, 1042-1046.
161. W. Wang, Y. X. Wang and H. B. Yang, *Chem. Soc. Rev.*, 2016, **45**, 2656-2693.
162. M. Fujita, O. Sasaki, T. Mitsuhashi, T. Fujita, J. Yazaki, K. Yamaguchi and K. Ogura, *Chem. Commun.*, 1996, 1535-1536.
163. J. M. Ludlow III, M. Tominaga, Y. Chujo, A. Schultz, X. Lu, T. Xie, K. Guo, C. N. Moorefield, C. Wesdemiotis and G. R. Newkome, *Dalton Trans.*, 2014, **43**, 9604-9611.
164. X. Lu, X. Li, K. Guo, T.-Z. Xie, C. N. Moorefield, C. Wesdemiotis and G. R. Newkome, *J. Am. Chem. Soc.*, 2014, **136**, 18149-18155.
165. T.-Z. Xie, K. J. Endres, Z. Guo, J. M. Ludlow III, C. N. Moorefield, M. J. Saunders, C. Wesdemiotis and G. R. Newkome, *J. Am. Chem. Soc.*, 2016, **138**, 12344-12347.
166. S. Chakraborty, K. J. Endres, R. Bera, L. Wojtas, C. N. Moorefield, M. J. Saunders, N. Das, C. Wesdemiotis and G. R. Newkome, *Dalton Trans.*, 2018, **in press**, DOI: 10.1039/C1037DT04571A.
167. T. Z. Xie, X. Wu, K. J. Endres, Z. Guo, X. Lu, J. Li, E. Manandhar, J. M. Ludlow III, C. N. Moorefield, M. J. Saunders, C. Wesdemiotis and G. R. Newkome, *J. Am. Chem. Soc.*, 2017, **139**, 15652-15655.
168. *USA Pat.,* US 20160222035, 2016.
169. Y.-R. Zheng, H.-B. Yang, K. Ghosh, L. Zhao and P. J. Stang, *Chem. Eur. J.*, 2009, **15**, 7203-7214.
170. I. Angurell, M. Ferrer, A. Gutiérrez, M. Martínez, L. Rodríguez, O. Rossell and M. Engeser, *Chem. Eur. J.*, 2010, **16**, 13960-13964.
171. Y.-R. Zheng, Z. Zhao, M. Wang, K. Ghosh, J. B. Pollock, T. R. Cook and P. J. Stang, *J. Am. Chem. Soc.*, 2010, **132**, 16873-16882.
172. Y. R. Zheng, W. J. Lan, M. Wang, T. R. Cook and P. J. Stang, *J. Am. Chem. Soc.*, 2011, **133**, 17045-17055.
173. M. L. Saha, S. Pramanik and M. Schmittel, *Chem. Commun.*, 2012, **48**, 9459-9461.
174. W. Meng, T. K. Ronson, J. K. Clegg and J. R. Nitschke, *Angew. Chem. Int. Ed.*, 2013, **52**, 1017-1021.
175. D. Samanta and P. S. Mukherjee, *Chem. Eur. J.*, 2014, **20**, 12483-12492.
176. J. R. Li and H. C. Zhou, *Nat. Chem.*, 2010, **2**, 893-898.
177. R. Sarkar, Z. Guo, J. Li, T. N. Burai, C. N. Moorefield, C. Wesdemiotis and G. R. Newkome, *Chem. Commun.*, 2015, **51**, 12851-12864.
178. A. Schultz, Y. Cao, M. Huang, S. Z. D. Cheng, X. Li, C. N. Moorefield, C. Wesdemiotis and G. R. Newkome, *Dalton Trans.*, 2012, **41**, 11573-11575.
179. D. Liu, Z. Jiang, M. Wang, X. Yang, H. Liu, M. Chen, C. N. Moorefield, G. R. Newkome and P. Wang, *Chem. Commun.*, 2016, **52**, 9773-9776.
180. Y. Li, Z. Jiang, J. Yuan, T. Wu, C. N. Moorefield, G. R. Newkome and P. Wang, *Chem. Commun.*, 2015, **51**, 5766-5769.
181. D. Liu, X. Yang, Y. Li and P. Wang, *Chem. Commun.*, 2016, **52**, 2513-2516.
182. S. Chakraborty, W. Hong, K. J. Endres, T.-Z. Xie, L. Wojtas, C. N. Moorefield, C. Wesdemiotis and G. R. Newkome, *J. Am. Chem. Soc.*, 2017, **139**, 3012-3020.
183. M. Chen, J. Wang, S. Chakraborty, D. Liu, Z. Jiang, Q. Liu, J. Yan, H. Zhong, G. R. Newkome and P. Wang, *Chem. Commun.*, 2017, **53**, 11087-11090.
184. L. Wang, Z. Zhang, X. Jiang, J. A. Irvin, C. Liu, M. Wang and X. Li, *Inorg. Chem.*, 2017, DOI: 10.1021/acs.inorgchem.7b02361.
185. M. D. Hager, P. Greil, C. Leyens, S. van der Zwaags and U. S. Schubert, *Adv. Mater.*, 2010, **22**, 5424-5430.
186. D. Zhao, S. Tan, D. Yuan, W. Lu, Y. H. Rezenom, H. Jiang, L. Q. Wang and H. C. Zhou, *Adv. Mater.*, 2011, **23**, 90-93.

187. E. Busseron, Y. Ruff, E. Moulin and N. Giuseppone, *Nanoscale*, 2013, **5**, 7098-7140.
188. X. Yan, F. Wang, B. Zheng and F. Huang, *Chem. Soc. Rev.*, 2012, **41**, 6042-6065.
189. A. Wild, A. Winter, F. Schlütter and U. S. Schubert, *Chem. Soc. Rev.*, 2011, **40**, 1459-1511.
190. V. Duprez, M. Biancardo, H. Spanggaard and F. C. Krebs, *Macromolecules*, 2005, **38**, 10436-10448.
191. P. Wang, C. N. Moorefield, S. Li, C. D. Shreiner, S.-H. Hwang and G. R. Newkome, *Chem. Commun.*, 2006, 1091-1093.
192. S.-H. Hwang, C. N. Moorefield, L. Dai and G. R. Newkome, *Chem. Mater.*, 2006, **18**, 4019-4024.
193. E. W. McQueen and J. I. Goldsmith, *J. Am. Chem. Soc.*, 2009, **131**, 17554-17556.
194. R. Siebert, A. Winter, M. Schmitt, J. Ã. Popp, U. S. Schubert and B. Dietzek, *Macromol. Rapid Commun.*, 2012, **33**, 481-497.
195. B. Rybtchinski, *ACS Nano*, 2011, **5**, 6791-6818.
196. N.-W. Wu, L.-J. Chen, C. Wang, Y.-Y. Ren, X. Li, L. Xu and H.-B. Yang, *Chem. Commun.*, 2014, **50**, 4231-4233.
197. X. Yan, S. Li, T. R. Cook, X. Ji, Y. Yao, J. B. Pollock, Y. Shi, G. Yu, J. Li, F. Huang and P. J. Stang, *J. Am. Chem. Soc.*, 2013, **135**, 14036-14039.
198. P. Wei, T. R. Cook, X. Yan, F. Huang and P. J. Stang, *J. Am. Chem. Soc.*, 2014, **136**, 15497-15500.
199. P. Wang, C. N. Moorefield, K.-U. Jeong, S.-H. Hwang, S. Li, S. Z. D. Cheng and G. R. Newkome, *Adv. Mater.*, 2008, **20**, 1381-1385.
200. Y.-T. Chan, C. N. Moorefield, M. Soler and G. R. Newkome, *Chem. Eur. J.*, 2010, **16**, 1768-1771.
201. J. M. Ludlow, M. J. Saunders, M. Huang, Z. Guo, C. N. Moorefield, S. Z. D. Cheng, C. Wesdemiotis and G. R. Newkome, *Supramol. Chem.*, 2017, **29**, 69-79.

**1**

## Graphical Abstract:

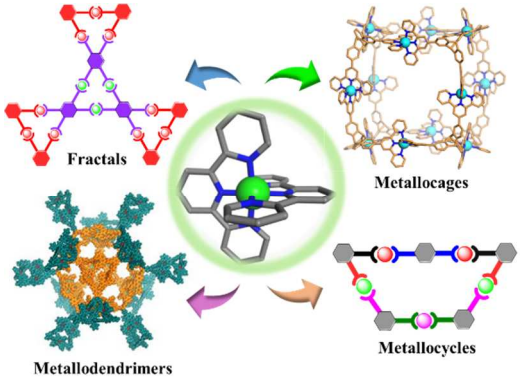


Comprehensive summary of the recent developments in the growing field of terpyridine-based, discrete metallosupramolecular architectures.